



MASTER OF SCIENCE IN ELECTRICAL AND ELECTRONIC ENGINEERING

Design and Analysis of a Wideband Microstrip Antenna for High Speed WLAN

S. M. Masudur Rahman Al-Arif

Department of Electrical and Electronic Engineering
Islamic University of Technology (IUT)
July, 2012

Design and Analysis of a Wideband Microstrip Antenna for High Speed WLAN

A Thesis Presented to the Academic Faculty

by

S. M. Masudur Rahman Al-Arif (102604)

In Partial Fulfillment of the Requirements for the Degree

MASTER OF SCIENCE
in
Electrical and Electronic Engineering

Islamic University of Technology
JULY 2012

The thesis titled

**DESIGN AND ANALYSIS OF A WIDEBAND MICRO-STRIP
ANTENNA FOR HIGH SPEED WLAN**

Submitted by S. M. Masudur Rahman Al-Arif St. No. 102604 of Academic Year 2010-2011 has been found as satisfactory and accepted as partial fulfillment of the requirement for the Degree Master Of Science in Electrical and Electronic Engineering.

Board of Examiners

Dr. Md. Fokhrul Islam, Supervisor
Assistant Professor, EEE Department
IUT, Gazipur - 1704

Chairman

Prof. Dr. Md. Shahid Ullah, (Ex-Officio)
Head and Professor, EEE Department
IUT, Gazipur - 1704

Member

Prof. Dr. Md. Ashraful Haque
Professor, EEE Department
IUT, Gazipur - 1704

Member

Prof. Dr. Mohammad Rakibul Islam
Professor, EEE Department
IUT, Gazipur - 1704

Member

Dr. Mohammed Imamul Hassan Bhuiyan
Associate Professor, EEE Department
BUET, Dhaka

Member (External)

Date Approved: 26.07.2012

Declaration of Candidate

It is here by declared that this thesis or any part of it has not been submitted elsewhere for the award of any Degree or Diploma.

Dr. Md. Fokhrul Islam, Supervisor
Assistant Professor, EEE Department
IUT, Gazipur – 1704

S. M. Masudur Rahman Al-Arif
Student Number: 102604
Academic Year: 2010-2011

TABLE OF CONTENTS

	Page
LIST OF FIGURES	v
LIST OF TABLES	viii
LIST OF SYMBOLS AND ABBREVIATIONS	viii
ACKNOWLEDGEMENTS	ix
ABSTRACT	x
<u>CHAPTER</u>	
1 INTRODUCTION	1
1.1. Wireless Local Area Network (WLAN)	1
1.2. Microstrip Patch Antenna	2
1.3. Contribution of the Thesis	4
1.4. Organisation of the Thesis	4
2 BACKGROUND	5
2.1. Antenna Characteristics	5
2.2. Characteristics of Basic Microstrip Patch Antenna	7
2.3. Analysis of Microstrip Patch Antenna	9
2.4. Feeding Techniques	20
2.5. Literature Review	23
3 PROPOSED ANTENNA	28
3.1. Specifications	28
3.2. Optimization	29
4 RESULTS AND SIMULATIONS	40
4.1. Average Current Distribution	42
4.2. Current Vector Distribution	44
4.3. 2D Radiation Pattern	46
4.4. 3D Radiation Pattern	48
4.5. Comparison of Designed Antenna with Existing Antennas	50
4.6. Insight into Parametric Study	51
5 CONCLUSION	53
APPENDIX A: RESONANCE FREQUENCY OF E- SHAPED ANTENNA	54
APPENDIX B: ANTENNA SIMULATION IN IE3D	57
APPENDIX C: MESHING PARAMETERS AND SIMULATION	62
REFERENCES	66

LIST OF FIGURES

	Page
Figure 2.1: Basic Microstrip Patch Antenna	7
Figure 2.2 (a): Transmission line model: Microstrip line	10
Figure 2.2 (b): Transmission line model: Electric field lines	10
Figure 2.3: Rectangular microstrip patch antenna	11
Figure 2.4 (a): Microstrip patch antenna: Top view	12
Figure 2.4 (b): Microstrip patch antenna: Side view	12
Figure 2.5: Charge Distribution and Current Density on Microstrip Patch	14
Figure 2.6: Microstrip Line Feed	20
Figure 2.7: Aperture-coupled Feed	21
Figure 2.8: Proximity-coupled Feed	21
Figure 2.9: Coaxial Probe Feed	22
Figure 2.10 (a): Equivalent circuits of Rectangular Patch	24
Figure 2.10 (b): Equivalent circuits of E shaped Microstrip Antennas	24
Figure 3.1: Primary Antenna	29
Figure 3.2: Return loss of the primary antenna	30
Figure 3.3: Increasing W	30
Figure 3.4: Frequency Response for W = 34, 36, 38 (mm)	31
Figure 3.5: Decreasing W	31
Figure 3.6: Frequency Response for W = 34, 32, 30, 28, 26, 24, 22 (mm)	32
Figure 3.7: Increasing W1	32
Figure 3.8: Frequency Response for W1 = 10, 12 (mm)	33
Figure 3.9: Decreasing W1	33
Figure 3.10: Frequency Response for W1 = 10, 8, 6, 5, 4 (mm)	34
Figure 3.11: Changing L from the top	34

LIST OF FIGURES

	Page
Figure 3.12: Frequency Response for L = 19, 18, 20 (mm)	35
Figure 3.13: Changing L from the bottom	35
Figure 3.14: Frequency Response for L = 19, 21, 18, 20 (mm)	36
Figure 3.15: Changing L1	36
Figure 3.16: Frequency Response for changing L1	37
Figure 3.17: Changing W2	37
Figure 3.18: Frequency Response for changing W2	38
Figure 3.19: Return loss for changing Ls	38
Figure 3.20: Final outcome with desired bandwidth	39
Figure 4.1: Structure view of the final antenna with dimension	40
Figure 4.2: Average Distribution of Current 5 GHz	42
Figure 4.3: Average Distribution of Current 5.25 GHz	42
Figure 4.4: Average Distribution of Current 5.5 GHz	43
Figure 4.5: Average Distribution of Current 5.775 GHz	43
Figure 4.6: Distribution of Current Vectors at 5 GHz	44
Figure 4.7: Distribution of Current Vectors at 5.25 GHz	44
Figure 4.8: Distribution of Current Vectors at 5.5 GHz	45
Figure 4.9: Distribution of Current Vectors at 5.775 GHz	45
Figure 4.10: 2D Radiation Pattern E-H fields at 5 GHz	46
Figure 4.11: 2D Radiation Pattern E-H fields at 5.25 GHz	46
Figure 4.12: 2D Radiation Pattern E-H fields at 5.5 GHz	47
Figure 4.13: 2D Radiation Pattern E-H fields at 5.775 GHz	47
Figure 4.14: 3D radiation pattern at 5 GHz	48

LIST OF FIGURES

	Page
Figure 4.15: 3D radiation pattern at 5.25 GHz	48
Figure 4.16: 3D radiation pattern at 5.5 GHz	49
Figure 4.17: 3D radiation pattern at 5.775 GHz	49
Figure 4.18: Parameters of rectangular antenna and E shaped patch antenna	51
Figure A-1: Diagram for equating the area of the E-Shaped antenna with RMSA	54
Figure B-1: Zeland Program Manager	57
Figure B-2: MGRID window	57
Figure B-3: Basic Parameter	58
Figure B-4: New Substrate Layer Dialog box	58
Figure B-5: Rectangle Dialog box	59
Figure B-6: Continue Straight Path Dialog box	59
Figure B-7: Main body of antenna with middle arm	60
Figure B-8: Antenna Structure with two arms	60
Figure B-9: Complete antenna structure	61
Figure B-10: Antenna Structure with feeding Probe	61
Figure C-1: Automatic Meshing Parameter dialog box	62
Figure C-2: Meshed Antenna for MoM calculation	63
Figure C-3: Simulation Setup dialog box	63
Figure C-4: Display Parameter	64
Figure C-5: Simulation Setup for Current Distribution and Radiation Pattern	65

LIST OF TABLES

	Page
Table 4.1: Summary of Parametric Study	52

LIST OF SYMBOLS AND ABBREVIATIONS

ϵ_r	Dielectric Constant
LAN	Local Area Network
WLAN	Wireless Local Area Network
Wi-Fi	A popular synonym for "WLAN"
GHz	Giga Hertz
IEEE	Institute of Electrical and Electronics Engineers
Mbits/s	Mega Bits per Second
MMIC	MilliMeter-wave Integrated Circuits
IE3D	Moment of Method Based EM Simulator
HTS	High Temperature Superconductor
PCB	Printed Circuit Board
3D	Three Dimensional
2D	Two Dimensional
BW	Bandwidth
RL	Return Loss
VSWR	Voltage Standing Wave Ratio
MIC	Microwave Integrated Circuits
Q	Quality Factor
RF	Radio Frequency

ACKNOWLEDGEMENTS

I express my sincere gratitude and indebtedness to the thesis supervisor **Dr. Md. Fokhrul Islam**, for his initiative in this field of research, for his valuable guidance, encouragement and affection for the successful completion of this work. His sincere sympathy and kind attitude always encouraged me to carry out the present work firmly. I express our thankfulness to **Prof. Dr. Md. Shahid Ullah**, Head of the Department of Electrical and Electronic Engineering, IUT, Gazipur for providing us with best facilities in the Department and his timely suggestions. I would also like to thank **Dr. Mohammed Imamul Hassan Bhuiyan**, Associate Professor, Department of Electrical and Electronic Engineering, BUET, Dhaka for his guidance and suggestions in our work.

Last but not least we would like to thank all my friends and well wishers who were involved directly or indirectly in successful completion of the present work.

S. M. MASUDUR RAHMAN AL ARIF

Student ID: 102604

DESIGN AND ANALYSIS OF A WIDEBAND MICRO-STRIP ANTENNA FOR HIGH SPEED WLAN

Abstract

The wired local area network is becoming wireless day by day. The allocation of frequency spectrum for this Wireless LAN is different in different countries. This presents a myriad of exciting opportunities and challenges for design in the communications arena, including antenna design. The high speed WLAN has many standards and most antennas available do not cover all the standards.

The objective in thesis is to design a suitable antenna that can be used for high speed WLAN application. The primary goal is to design antenna with smallest possible size and better polarization that covers all the high speed WLAN standards ranging from 4.90 GHz to 5.82 GHz.

Many works are going on throughout the world in field of antenna designing. Recent works on this field is studied in this thesis to find out most suitable antenna shape for the specific application. Zeland's IE3D simulation software has been used to design and simulate antenna for WLAN frequency band. A parametric study has been presented in process to the designed antenna for an effective bandwidth of 4.9-5.825 GHz. Return loss -10 dB or lower is taken as acceptable limit.

Finally single E shape microstrip patch antenna having a dimension of 24×19 mm² is demonstrated with a frequency band of 4.89 GHz to 5.83 GHz. The antenna presents a good current distribution and radiation pattern for all four standards of WLAN that falls inside this frequency range.

CHAPTER 1

INTRODUCTION

1.1 Wireless Local Area Network (WLAN)

Wireless local area network (WLAN) is a technology that links two or more devices using wireless distribution method and usually providing a connection to the wider internet. This gives users the mobility to move around within a local coverage area and still be connected to the network. WLANs have become popular in the home due to ease of installation and in commercial complexes offering wireless access to their customers; often for free. Large wireless network projects are being put up in many major cities around the globe. Most modern WLANs are based on IEEE 802.11 standards, marketed under the Wi-Fi brand name.

WLANs are used worldwide and at different region of world different frequency bands are used. The first generation WLANs IEEE 802.11b and IEEE 802.11g standards utilize the 2.4 GHz band [1]. It supports relatively low data rates, just up to 10 Mbits/s compared with wired counterparts. In most cases this frequency band is license-free, hence the WLAN equipment of this band suffers interference from other devices that use this same band. The current fastest and robust WLAN standard IEEE 802.11a operate in the 5–6 GHz band, which can provide reliable high-speed connectivity up to 54 Mbits/s. The 802.11a standard is much cleaner and developed to support high-speed WLAN. But USA, Europe and some other countries use different frequency bands for this high speed 802.11a standard. Among the two popular bands used for IEEE 802.11a standard; USA uses 5.15–5.35 GHz band and Europe uses 5.725–5.825 GHz band. Some countries allow the operation in the 5.47–5.825GHz band. Another new band of 4.9–5.1 GHz has been proposed for WLAN system as IEEE 802.11j in Japan [1]. Most of the current antennas available at the point supports only one or at max two of those standards. So people have to use different transceivers for different region because of this variety of frequency band unless we can design an antenna that can cover the whole high speed WLAN range of 4.9 – 5.825 GHz. Our main objective in this thesis is to find a suitable antenna that can do so.

Different kind antennas and their suitability in the WLAN applications have been studied throughout the literature review. Finally a coaxial probe fed, single stacked, E – shaped microstrip patch antenna has been chosen for the specific case. Then an exhaustive parametric study has been performed on the antenna in order to optimize the antenna for the mentioned wide bandwidth. An antenna with a bandwidth of 925 MHz starting from 4.890 GHz to 5.825 GHz and size of 26×19 mm² is found which is much smaller than other available antennas. As the main objective is satisfied, simulations for current distribution and radiation patterns have been examined at different frequencies inside that bandwidth to observe the antennas behavior on the whole frequency. Then a brief comparison with other available antenna with the proposed antenna is described along with a summary of the parametric study. Finally scopes for future works are mentioned in conclusion.

1.2 Microstrip Patch Antenna

In recent years, the current trend in commercial and government communication systems has been to develop low cost, minimal weight, low profile antennas that are capable of maintaining high performance over a large spectrum of frequencies. This technological trend has focused much effort into the design of microstrip patch antennas. With a simple geometry, patch antennas offer many advantages not commonly exhibited in other antenna configurations. For example, they are extremely low profile, lightweight, simple and inexpensive to fabricate using modern day printed circuit board technology, compatible with microwave and millimeter-wave integrated circuits (MMIC) and have the ability to conform to planar and non-planar surfaces. In addition, once the shape and operating mode of the patch are selected, designs become very versatile in terms of operating frequency, polarization, pattern, and impedance. The variety in design that is possible with microstrip antennas probably exceeds that of any other type of antenna element. However, standard rectangular microstrip patch antenna also has the drawbacks of narrow bandwidth. Researchers have made many efforts to overcome this problem and many configurations have been presented to extend the bandwidth.

Our primary objective is to find out the most suitable antenna shape applicable to be used in the multi-standard WLAN applications around the globe. Different shapes and their use in various fields of wireless communications [1-12] have been studied in the literature review portion. The most suitable shape for WLAN application based on different advantages and disadvantages mentioned in the literatures is found through the study.

Once the most suitable shape is found, an antenna is chosen based on the best option available for the WLAN band. Then the antenna is designed in IE3D simulation software. IE3D is a general purpose electromagnetic simulation and optimization package that has been developed for the design and analysis of planar and 3D structures encountered in microwave and MMIC, high temperature superconductor (HTS) circuits, microstrip antennas, Radio frequency (RF) printed circuit board (PCB) and high speed digital circuit packaging. Based upon an integral equation, method of moment (MoM) algorithm, the simulator can accurately and efficiently simulate arbitrarily shaped and oriented 3D metallic structures in multi-layer dielectric substrates. It is very popular and recognized software for antenna simulation. This software can be used to examine different parameters, 2D, 3D radiation patterns and current distributions inside the antenna. We can also easily compare the output of different antennas in the same graph/window allowing us to take decisions regarding the best antenna.

Then IE3D is used to carry out a comprehensive parametric study to understand the effects of various dimensional parameters and to optimize the performance of the antenna. An insight on how different design parameter affects operating frequency, bandwidth and other output parameters is also found. Finally based on the comparison we can select a perfect antenna for WLAN application with wider bandwidth and multi-band capability.

1.3 Contribution of the Thesis

An antenna for high speed WLAN standards covering a bandwidth from 4.90 GHz to 5.82 GHz has been designed and simulated in this thesis. A parametric study of E shape antenna has also been presented which can be very useful to understand the effects of various parameters on the bandwidth.

1.4 Organisation of the Thesis

The dissertation is mainly divided into five chapters. Introduction to WLAN, microstrip antenna and main objectives of the thesis have already been expressed in Chapter 1.

Chapter 2 provides some information about basic properties of antenna and the literature review done in the process. Based on the literature review an antenna is taken for optimization. Optimization is done by simulating the antenna with variable parameters. The effects of this parametric study and the final optimized design are discussed in Chapter 3.

The average and vector current distributions, 2D and 3D radiation patterns of the final optimized antenna for all basic 802.11 standards in 5-6GHz range are shown and discussed in Chapter 4. Also the effects of parametric study have been summarized to understand the effect of different parameters on bandwidth, resonance and return loss. A comparison with existing antennas and proposed antenna is also briefly discussed in this chapter.

Finally conclusive discussion and scope for future works are described in the fifth and the final chapter.

CHAPTER 2

BACKGROUND

2.1 Antenna Characteristics

An antenna is an electrical device which converts electric currents into radio waves, and vice versa. It is usually used with a radio transmitter or radio receiver. In transmission, a radio transmitter applies an oscillating radio frequency electric current to the antenna's terminals, and the antenna radiates the energy from the current as electromagnetic waves (radio waves). In reception, an antenna intercepts some of the power of an electromagnetic wave in order to produce a tiny voltage at its terminals, which is applied to a receiver to be amplified. An antenna can be used for both transmitting and receiving. So in short, antenna is a device that is made to efficiently radiate and receive radiated electromagnetic waves. There are several important antenna characteristics that should be considered when choosing an antenna for any particular application such as:

- Bandwidth (BW)
- Return Loss (RL)
- Gain
- VSWR
- Radiation Pattern
- Polarization

Input impedance is an important characteristic of antenna. For an efficient transfer of energy, impedances of all the elements must match each other or in other words impedance of the radio, of the antenna and of the transmission cable connecting them must be the same. Transceivers and their transmission lines are typically designed for particular impedance. If the antenna has impedance different from that, then there is a mismatch and an impedance matching circuit is required.

An antenna's bandwidth specifies the range of frequencies over which its performance does not suffer due to a poor impedance match.

When a signal is fed into an antenna, the antenna will emit radiation distributed in space in a certain way. A graphical representation of the relative distribution of the radiated power in space is called a radiation pattern. The radiation pattern describes the relative strength of the radiated field in various directions from the antenna, at a constant distance. The radiation pattern is a reception pattern as well, since it also describes the receiving properties of the antenna. The radiation pattern is three-dimensional, but usually the measured radiation patterns are a two-dimensional slice of the three-dimensional pattern, in the horizontal or vertical planes. These pattern measurements are presented in either a rectangular or a polar format.

Gain is a parameter which measures the degree of directivity of the antenna's radiation pattern. A high-gain antenna will preferentially radiate in a particular direction. Specifically, the antenna gain, or power gain of an antenna is defined as the ratio of the intensity (power per unit surface) radiated by the antenna in the direction of its maximum output, at an arbitrary distance, divided by the intensity radiated at the same distance by a hypothetical isotropic antenna.

As an electro-magnetic wave travels through the different parts of the antenna system it may encounter differences in impedance. At each interface, depending on the impedance match, some fraction of the wave's energy will reflect back to the source, forming a standing wave in the feed line. The ratio of maximum power to minimum power in the wave can be measured and is called the standing wave ratio (SWR). The SWR is usually defined as a voltage ratio called the VSWR. The VSWR is always a real and positive number for antennas. The smaller the VSWR is, the better the antenna is matched to the transmission line and the more power is delivered to the antenna. The minimum VSWR is 1.0. In this case, no power is reflected from the antenna, which is ideal. As the VSWR increases, there are 2 main drawbacks. The first is obvious: more power is reflected from the antenna and therefore not transmitted. However, another problem arises. As VSWR

increases, more power is reflected to the radio, which is transmitting. Large amounts of reflected power can damage the radio. Usually a VSWR of ≤ 2 is acceptable for antennas. The return loss (RL) is another way of expressing mismatch. It is a logarithmic ratio measured in dB that compares the power reflected by the antenna to the power that is fed into the antenna from the transmission line. The RL is directly related with the VSWR.

$$RL = -20 \log \left(\frac{VSWR - 1}{VSWR + 1} \right) \text{ dB}$$

In practice, the most commonly quoted parameter in regards to antennas is S_{11} . S_{11} is actually nothing but the return loss (RL). If $S_{11} = 0$ dB, then all the power is reflected from the antenna and nothing is radiated. If $S_{11} = -10$ dB, this implies that if 3 dB of power is delivered to the antenna, -7 dB is the reflected power. The acceptable VSWR of ≤ 2 corresponds to a RL or S_{11} of -9.5 dB or lower. In this thesis RL of -10 dB or lower is taken as acceptable.

2.2 Characteristics of Basic Microstrip Patch Antenna

In its basic form, a Microstrip Patch antenna consists of a radiating patch on one side of a dielectric substrate which has a ground plane on the other side as shown in Figure 2.1.

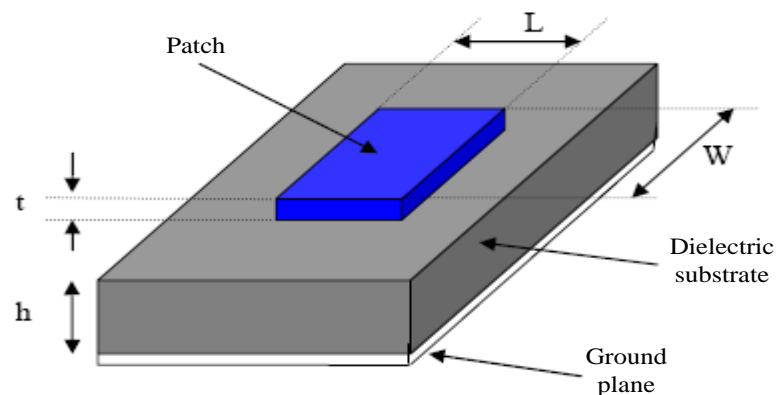


Figure 2.1: Basic Microstrip Patch Antenna

The patch is normally made of conducting material such as copper or gold and can take any possible shape. The radiating patch and the feed lines are usually photo etched on the dielectric substrate. In order to simplify analysis and performance estimation, generally square, rectangular, circular, triangular, and elliptical or some other common shape patches are used for designing a microstrip antenna. In our case we are going to design E shape patch antenna because of its dual resonating characteristics which results in wider bandwidth. The microstrip patch antennas radiate primarily because of the fringing fields between the patch edge and the ground plane. For good performance of antenna, a thick dielectric substrate having a low dielectric constant is necessary since it provides larger bandwidth, better radiation and better efficiency. However, such a typical configuration leads to a larger antenna size. In order to reduce the size of the Microstrip patch antenna, substrates with higher dielectric constants must be used which are less efficient and result in narrow bandwidth. Hence a trade-off must be realized between the antenna performance and antenna dimensions.

Microstrip patch antennas are mostly used in wireless applications due to their low- profile structure. Therefore they are extremely compatible for embedded antennas in handheld wireless devices such as cellular phones, pagers etc.

Some of the principal advantages are given below:

- Light weight and less volume;
- Low fabrication cost, therefore can be manufactured in large quantities;
- Supports both, linear as well as circular polarization;
- Low profile planar configuration;
- Can be easily integrated with microwave integrated circuits (MICs);
- Capable of dual and triple frequency operations;
- Mechanically robust when mounted on rough surfaces;

Some of their major disadvantages are given below:

- Narrow bandwidth;
- Low efficiency;
- Low gain;
- Low power handling capacity etc.

Microstrip patch antennas also have a very high antenna quality factor (Q). It represents the losses associated with the antenna where a large Q leads to narrow bandwidth and low efficiency. Q can be decreased by increasing the thickness of the dielectric substrate. But as the thickness increases, an increasing fraction of the total power delivered by the source goes into a surface wave. This surface wave contribution can be counted as an unwanted power loss since it is ultimately scattered at the dielectric bends and causes degradation of the antenna characteristics.

2.3 Analysis of Microstrip Patch Antenna

The most popular models for the analysis of microstrip patch antennas are the transmission line model, cavity model, and full wave model. The transmission line model is the simplest of all and it gives good physical insight but it is less accurate. The cavity model is more accurate and gives good physical insight but is complex in nature. The full wave models are extremely accurate, versatile and can treat single elements, finite and infinite arrays, stacked elements, arbitrary shaped elements and coupling. These give less insight as compared to the two models mentioned above and are far more complex in nature.

2.3.1 Transmission Line Model

This model represents the microstrip antenna by two slots of width W and height h , separated by a transmission line of length L as shown in Figure 2.2 (a). The

microstrip is essentially a nonhomogeneous line of two dielectrics, typically the substrate and air. Hence, as seen from Figure 2.2 (b), most of the electric field lines reside in the substrate and parts of some lines in air.

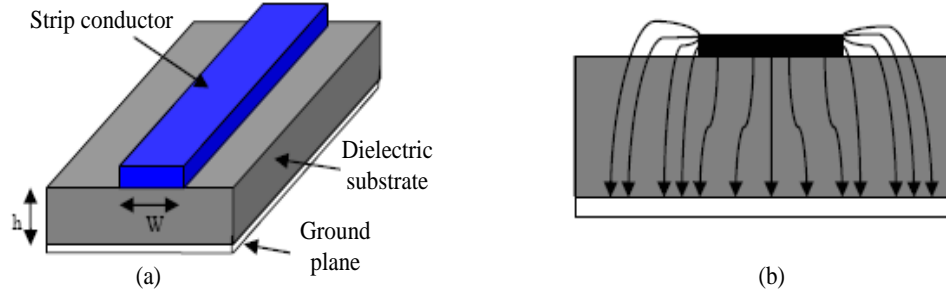


Figure 2.2: Transmission line model a) microstrip line and b) electric field lines [14]

As a result, this transmission line cannot support pure TEM mode of transmission, since the phase velocities would be different in the air and the substrate. Instead, the dominant mode of propagation would be the quasi-TEM mode. Hence, an effective dielectric constant (ϵ_{r_eff}) must be obtained in order to account for the fringing and the wave propagation in the line. The value of ϵ_{r_eff} is slightly less than ϵ_r because the fringing fields around the periphery of the patch are not confined in the dielectric substrate but are also spread in the air as shown in Figure 2.2 above. The expression for ϵ_{r_eff} is given by [14]:

$$\epsilon_{r_eff} = \frac{\epsilon_r + 1}{2} + \frac{\epsilon_r - 1}{2} \left[1 + 12 \frac{h}{W} \right]^{-\frac{1}{2}} \quad 2.1$$

where

ϵ_{r_eff} = Effective dielectric constant

ϵ_r = Dielectric constant of substrate

h = Height of dielectric substrate

W = Width of patch

Consider Figure 2.3 below, which shows a rectangular microstrip patch antenna of length L , width W resting on a substrate of height h . The co-ordinate axis is selected such that the length is along the x direction, width is along the y direction and the height is along the z direction.

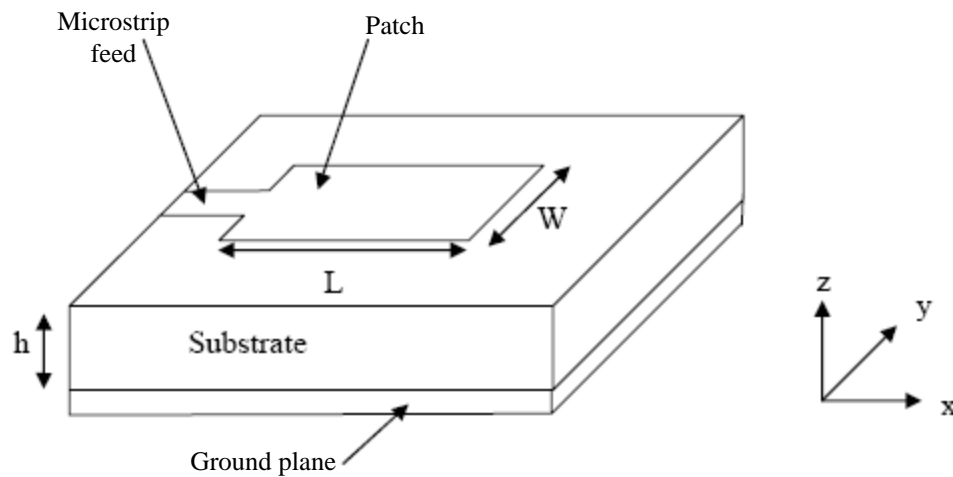


Figure 2.3: Rectangular microstrip patch antenna [15]

In order to operate in the fundamental TM_{10} mode, the length of the patch must be slightly less than $\lambda/2$ where λ is the wavelength in the dielectric medium and is equal to $\lambda_0/\sqrt{\epsilon_{r_eff}}$ where λ_0 is the free space wavelength. The TM_{10} mode implies that the field varies one $\lambda/2$ cycle along the length, and there is no variation along the width of the patch. In the Figure 2.4 (a), the microstrip patch antenna is represented by two slots, separated by a transmission line of length L and open circuited at both the ends. Along the width of the patch, the voltage is maximum and current is minimum due to the open ends. The fields at the edges can be resolved into normal and tangential components with respect to the ground plane.

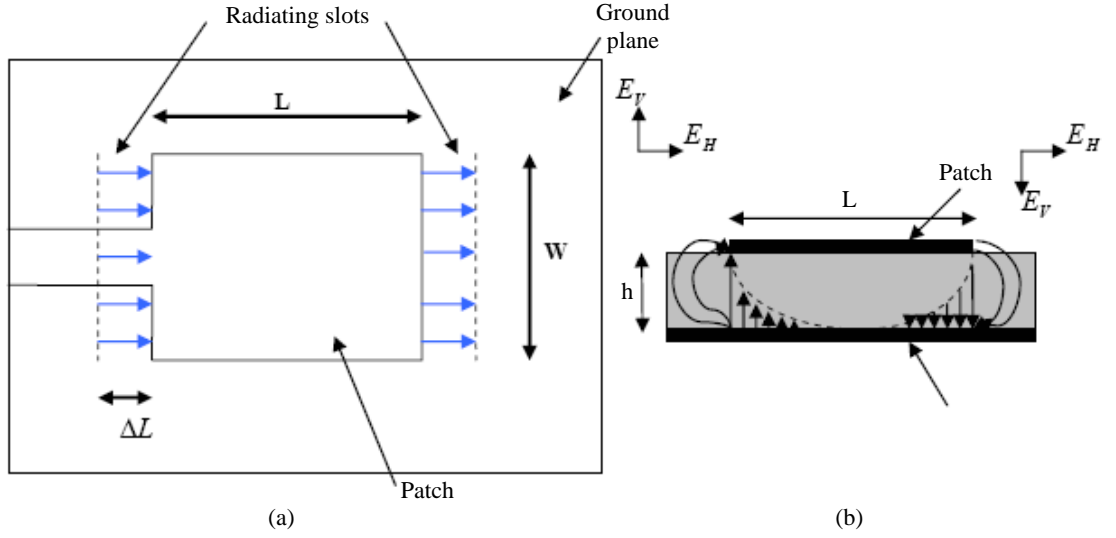


Figure 2.4: Microstrip patch antenna a) top view and b) side view [15]

It is seen from Figure 2.4 (b) that the normal components of the electric field at the two edges along the width are in opposite directions and thus out of phase since the patch is $\lambda/2$ long and hence they cancel each other in the broadside direction. The tangential components (seen in Figure 2.4 (b)), which are in phase, means that the resulting fields combine to give maximum radiated field normal to the surface of the structure. Hence the edges along the width can be represented as two radiating slots, which are $\lambda/2$ apart and excited in phase and radiating in the half space above the ground plane. The fringing fields along the width can be modeled as radiating slots and electrically the patch of the microstrip antenna looks greater than its physical dimensions. The dimensions of the patch along its length have now been extended on each end by a distance ΔL , which is given empirically by [15]:

$$\Delta L = 0.412h \frac{(\epsilon_{r_eff} + 0.3) \left(\frac{W}{h} + 0.264 \right)}{(\epsilon_{r_eff} - 0.258) \left(\frac{W}{h} + 0.8 \right)} \quad 2.2$$

The effective length of the patch L_{eff} now becomes

$$L_{eff} = L + 2\Delta L \quad 2.3$$

For a given resonance frequency f_0 , the effective length is given by [16]:

$$L_{eff} = \frac{c}{2f_0\sqrt{\epsilon_{r_eff}}} \quad 2.4$$

For a rectangular microstrip patch antenna, the resonance frequency for any TM_{mn} mode is given by [16]:

$$f_0 = \frac{c}{2\sqrt{\epsilon_{r_eff}}} \left[\left(\frac{m}{L} \right)^2 + \left(\frac{n}{W} \right)^2 \right]^{\frac{1}{2}} \quad 2.5$$

where m and n are modes along L and W respectively.

For efficient radiation, the width W is given by [16]

$$W = \frac{c}{2f_0\sqrt{\frac{(\epsilon_r + 1)}{2}}} \quad 2.6$$

2.3.2 Cavity Model

Although the transmission line model discussed in the previous section is easy to use, it has some inherent disadvantages. Specifically, it is useful for patches of rectangular design and it ignores field variations along the radiating edges. These disadvantages can be overcome by using the cavity model. In this model, the interior region of the dielectric substrate is modeled as a cavity bounded by electric walls on the top and bottom. The basis for this assumption is the following observations for thin substrates ($h \ll \lambda$) [17]. Since the substrate is thin, the fields in the interior region do not vary much in the z direction, i.e. normal to the patch. The electric field is z directed only, and the magnetic field has only the transverse components H_x and H_y in the region bounded by the patch metallization and the ground plane. This observation provides for the electric walls at the top and the bottom.

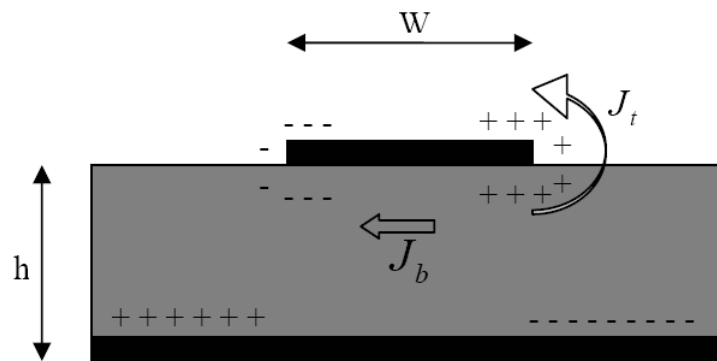


Figure 2.5: Charge distribution and current density on microstrip patch [17]

Consider Figure 2.5 shown above. When the microstrip patch is provided power, a charge distribution is seen on the upper and lower surfaces of the patch and at the bottom of the ground plane. This charge distribution is controlled by two mechanisms an attractive mechanism and a repulsive mechanism as discussed by [18]. The attractive mechanism is between the opposite charges on the bottom side of the patch and the ground plane, which helps in keeping the charge concentration intact at the bottom of the patch. The repulsive mechanism is between the like charges on the bottom surface of the patch, which causes pushing of some charges from the bottom, to the top of the patch. As a result of this charge movement, currents flow at the top and bottom surface of the patch. The cavity model assumes that the height to width ratio (i.e. height of substrate and width of the patch) is very small and as a result of this the attractive mechanism dominates and causes most of the charge concentration and the current to be below the patch surface. Much less current would flow on the top surface of the patch and as the height to width ratio further decreases, the current on the top surface of the patch would be almost equal to zero, which would not allow the creation of any tangential magnetic field components to the patch edges. Hence, the four sidewalls could be modeled as perfectly magnetic conducting surfaces. This implies that the magnetic fields and the electric field distribution beneath the patch would not be disturbed. However, in practice, a finite width to height ratio would be there and this would not make the tangential magnetic fields to be completely zero, but they being very small, the side walls could be approximated to be perfectly magnetic conducting [19].

Since the walls of the cavity, as well as the material within it are lossless, the cavity would not radiate and its input impedance would be purely reactive. Hence, in order to account for radiation and a loss mechanism, one must introduce a radiation resistance R_r and a loss resistance R_l . A lossy cavity would now represent an antenna and the loss is taken into account by the effective loss tangent δ_{eff} which is given as

$$\delta_{eff} = 1/Q_T \quad 2.7$$

Q_T is the total antenna quality factor and has been expressed by [16] in the form

$$\frac{1}{Q_T} = \frac{1}{Q_d} + \frac{1}{Q_c} + \frac{1}{Q_r} \quad 2.8$$

Q_d represents the quality factor of the dielectric and is given by

$$Q_d = \frac{\omega_r W_T}{P_d} = \frac{1}{\tan \delta} \quad 2.9$$

where

ω_r is the angular resonant frequency

W_T is the total energy stored in the patch at resonance

P_d is the dielectric loss

$\tan \delta$ is the loss tangent of the dielectric

Q_c represents the quality factor of the conductor and is given by

$$Q_c = \frac{\omega_r W_T}{P_c} = \frac{h}{\Delta} \quad 2.10$$

where

P_c is the conductor loss

Δ is the skin depth of the conductor

h is the height of the substrate

Q_r represents the quality factor for radiation and is given by

$$Q_r = \frac{\omega_r W_T}{P_r} \quad 2.11$$

where P_r is the power radiated from the patch.

Substituting equations 2.8, 2.9, 2.10 and 2.11 in equation 2.7, it found that

$$\delta_{eff} = \tan \delta + \frac{\Delta}{h} + \frac{P_r}{\omega_r W_T} \quad 2.12$$

Thus, equation 2.12 describes the total effective loss tangent for the microstrip patch antenna.

2.3.3 Full Wave Solutions-Method of Moments

One of the methods, that provide the full wave analysis for the microstrip patch antenna, is the Method of Moments. In this method, the surface currents are used to model the microstrip patch and the volume polarization currents are used to model the fields in the dielectric slab. It has been shown by [17], how an integral equation is obtained for these unknown currents and using the Method of Moments, these electric field integral equations are converted into matrix equations which can then be solved by various techniques of algebra to provide the result. The basic form of the equation to be solved by the Method of Moment is

$$F(g) = h \quad 2.13$$

where F is a known linear operator, g is an unknown function, and h is the source or excitation function. The aim here is to find g , when F and h are known. The unknown function g can be expanded as a linear combination of N terms given by

$$g = \sum_{n=1}^N a_n g_n = a_1 g_1 + a_2 g_2 + \dots + a_N g_N \quad 2.14$$

where a_n is an unknown constant and g_n is a known function usually called a basis or expansion function. Using the linearity property of the operator F , it can be present by

$$\sum_{n=1}^N a_n F(g_n) = h \quad 2.15$$

The basis functions g_n must be selected in such a way, that each $F(g_n)$ in the above equation 2.15 can be calculated. The unknown constants a_n cannot be determined directly because there are N unknowns, but only one equation. One method of finding these constants is the method of weighted residuals. In this method, a set of trial solutions is established with one or more variable parameters. The residuals are a measure of the difference between the trial solution and the true solution. The variable parameters are selected in a way which guarantees a best fit of the trial functions based on the minimization of the residuals. This is done by defining a set of N weighting (or testing) functions $\{w_m\} = w_1, w_2, \dots, w_n$ in the domain of the operator F . Taking the inner product of these functions, equation 2.15 becomes

$$\sum a_n \langle w_m, F(g_n) \rangle = \langle w_m, h \rangle \quad 2.16$$

where $m = 1, 2, \dots, N$

Writing in matrix form as shown in [14]

$$[F_{mn}][a_n] = [h_m] \quad 2.17$$

where

$$[F_{mn}] = \begin{bmatrix} \langle w_1, F(g_1) \rangle \langle w_1, F(g_2) \rangle \cdots \cdots \\ \langle w_2, F(g_1) \rangle \langle w_2, F(g_2) \rangle \cdots \cdots \\ \vdots \\ \vdots \end{bmatrix} \quad [a_n] = \begin{bmatrix} a_1 \\ a_2 \\ a_3 \\ \vdots \\ a_N \end{bmatrix} \quad [h_m] = \begin{bmatrix} \langle w_1, h \rangle \\ \langle w_2, h \rangle \\ \langle w_3, h \rangle \\ \vdots \\ \langle w_N, h \rangle \end{bmatrix}$$

The unknown constants a_n can now be found using algebraic techniques such as LU decomposition or Gaussian elimination. It must be remembered that the weighting functions must be selected appropriately so that elements of $\{w_n\}$ are not only linearly independent but they also minimize the computations required to evaluate the inner product. One such choice of the weighting functions may be to let the weighting and the basis function be the same, that is, $w_n = g_n$. This is called as the Galerkin's Method as described by [14]. From the antenna theory point of view, it can write the Electric field integral equation as

$$E = f_e(J) \quad 2.18$$

where

E is the known incident electric field

J is the unknown induced current

f_e is the linear operator

The first step in the moment method solution process would be to expand J as a finite sum of basis function given by

$$J = \sum_{i=1}^M J_i b_i \quad 2.19$$

where b_i is the i th basis function and J_i is an unknown coefficient. The second step involves the defining of a set of M linearly independent weighting functions, w_j . Taking the inner product on both sides and substituting equation 2.19 in equation 2.18, can be present by

$$\langle w_j, E \rangle = \sum_{i=1}^M \langle w_j, f_e(J_i, b_i) \rangle \quad 2.20$$

where $j = 1, 2, \dots, M$

Writing in Matrix form as,

$$[Z_{ij}] [J] = [E_j] \quad 2.21$$

where

$$Z_{ij} = \langle w_j, f_e(b_i) \rangle$$

$$E_j = \langle w_j, H \rangle$$

J is the current vector containing the unknown quantities.

The vector E contains the known incident field quantities and the terms of the Z matrix are functions of geometry. The unknown coefficients of the induced current are the terms of the J vector. Using any of the algebraic schemes mentioned earlier, these equations can be solved to give the current and then the other parameters such as the scattered electric and magnetic fields can be calculated directly from the induced currents. Thus, the moment method has been briefly explained for use in antenna problems. The software used in this thesis, Zeland Inc's IE3D (2007) is a moment method simulator [20].

2.4 Feeding Techniques

Microstrip patch antennas can be fed by a variety of methods. These methods can be classified into two categories- contacting and non-contacting. In the contacting method, the RF power is fed directly to the radiating patch using a connecting element such as a microstrip line. In the non-contacting scheme, electromagnetic field coupling is done to transfer power between the microstrip line and the radiating patch. The four most popular feed techniques used are the microstrip line, coaxial probe (both contacting schemes), aperture coupling and proximity coupling (both non-contacting schemes).

In microstrip line feed technique, a conducting strip is connected directly to the edge of the microstrip patch. The conducting strip is smaller in width as compared to the patch and this kind of feed arrangement has the advantage that the feed can be etched on the same substrate to provide a planar structure. But this feeding technique leads to undesired cross polarized radiation and spurious feed radiation which as a result hampers the bandwidth.

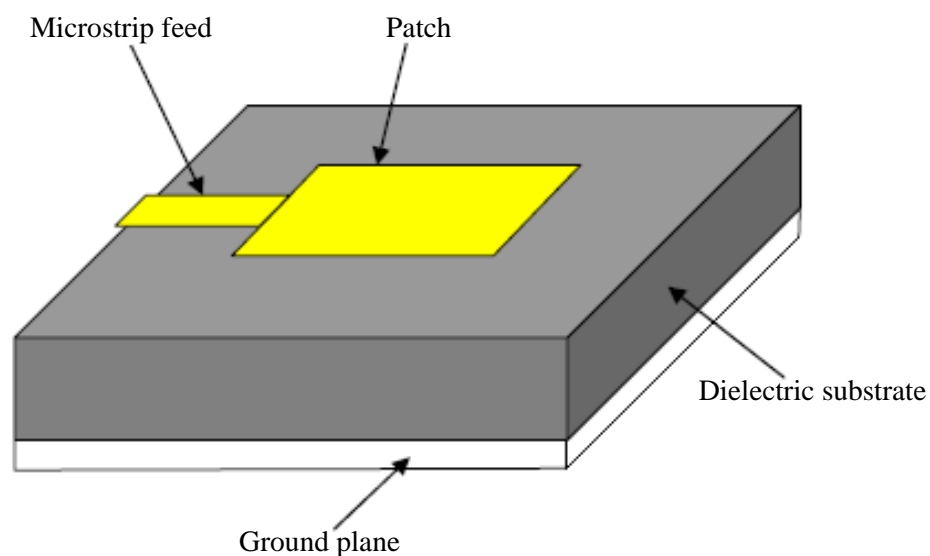


Figure 2.6: Microstrip Line Feed

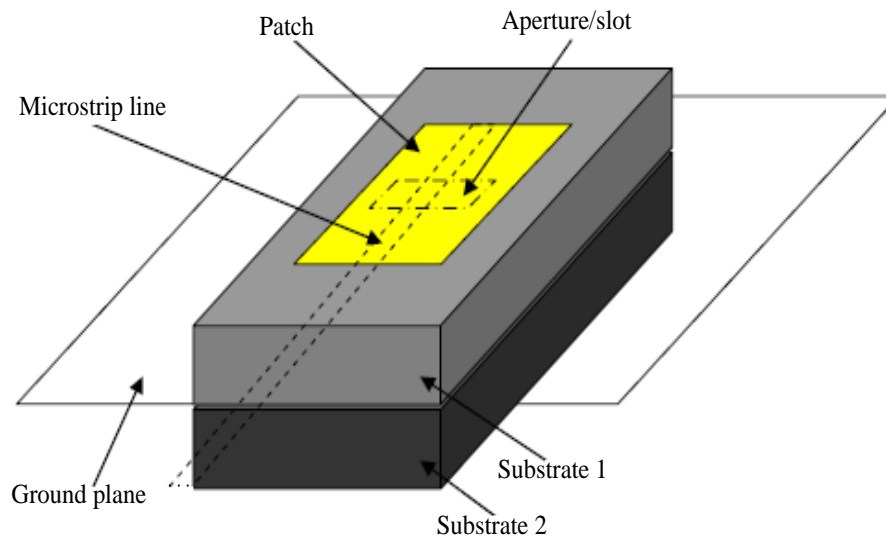


Figure 2.7: Aperture-coupled Feed

In aperture coupled feed technique coupling between the patch and the feed line is made through a slot or an aperture in the ground plane. Both cross-polarization and spurious radiation are minimized in this feeding technique. The major disadvantage of this feed technique is that it is difficult to fabricate due to multiple layers, which also increases the antenna thickness. This feeding scheme also provides narrow bandwidth.

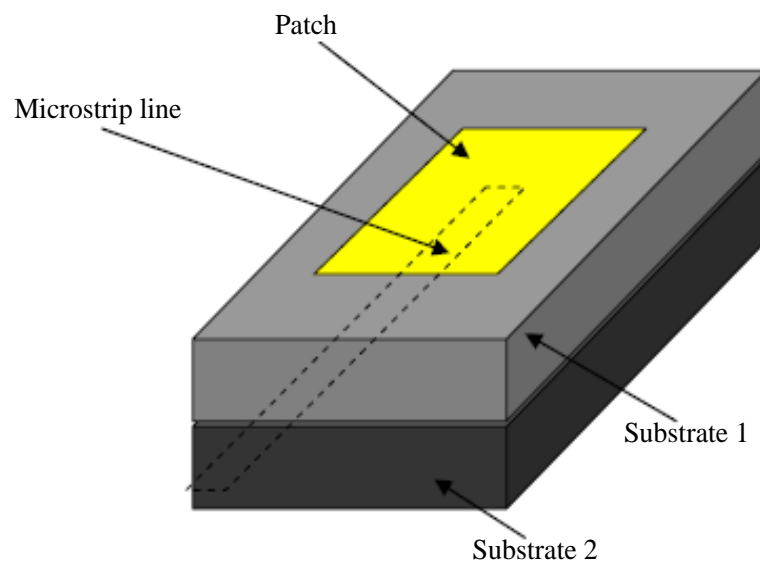


Figure 2.8: Proximity-coupled Feed

In Proximity coupled feed, two dielectric substrates are used such that the feed line is between the two substrates and the radiating patch is on top of the upper substrate. The main advantage of this feed technique is that it eliminates spurious feed radiation and provides very high bandwidth. But it is difficult to fabricate because of the two dielectric layers which need proper alignment. Also, there is an increase in the overall thickness of the antenna.

The Coaxial feed or probe feed is a very common technique used for feeding microstrip patch antennas. As seen from Figure 2.9, the inner conductor of the coaxial connector extends through the dielectric and is soldered to the radiating patch, while the outer conductor is connected to the ground plane. The main advantage of this type of feeding scheme is that the feed can be placed at any desired location inside the patch in order to match with its input impedance. This feed method is easy to fabricate and has low spurious radiation. Among all these feeding techniques coaxial probe feed has been chosen for the proposed antenna for its advantages.

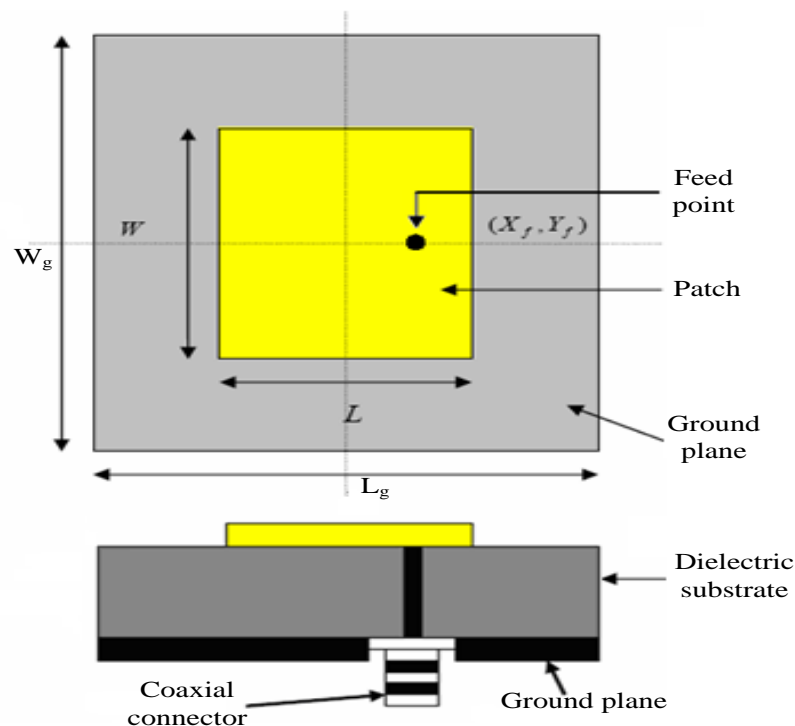


Figure 2.9: Coaxial Probe Feed

Generally for a rectangular patch antenna resonant length determines the resonant frequency. But for specially modified patches like U shape, V shape and E shape patches the relation between the resonant frequency and length or width becomes much complex because their multiple resonance characteristics and complex geometry.

2.5 Literature Review

As mentioned earlier although the microstrip patch antenna has a lot of advantages but it also has the drawback of narrow bandwidth. Many researchers have been working to increase the bandwidth of microstrip antenna. It has been observed that the bandwidth of microstrip antenna may be increased by using air substrate [2], increasing the substrate thickness, introducing parasitic patches element either in co-planar or stack configuration. In [3], an aperture-coupled microstrip antenna is described with parasitic patches stacked on the top of the main patch. However, all these methods typically enlarge the antenna size, either in the antenna plane or in the antenna height. Another very popular way to increase bandwidth of single patch antenna is to modify the shape of a common radiator patch by cutting slots strategically in the metallic patch. This approach is particularly attractive because it can provide excellent bandwidth improvement and maintain a single-layer radiating structure to preserve the antenna's thin profile characteristic. The successful examples include U-slot patch antennas [4], Half U shape antenna or L shape [5], V-slot patch antennas [6], double-C patch antennas [7] and E-shaped patch antennas [1, 8-11].

Recently in a study [4], it was shown that a half U-slot patch antenna maintains similar wide-band behavior like the full U-slot patch. In [5] it was shown that modifying the U-slot to a truncated V-slot can improve the antenna bandwidth considerably. Double C path antennas have been used commercially since 1995 [7]. But among all the shapes E shapes have gained most of the popularities because of its simplicity and robustness. When two parallel slots are incorporated into the

antenna patch to form a E shape, the bandwidth increases significantly.

The E-shaped patch is formed by inserting a pair of wide slits at the boundary of a microstrip patch.

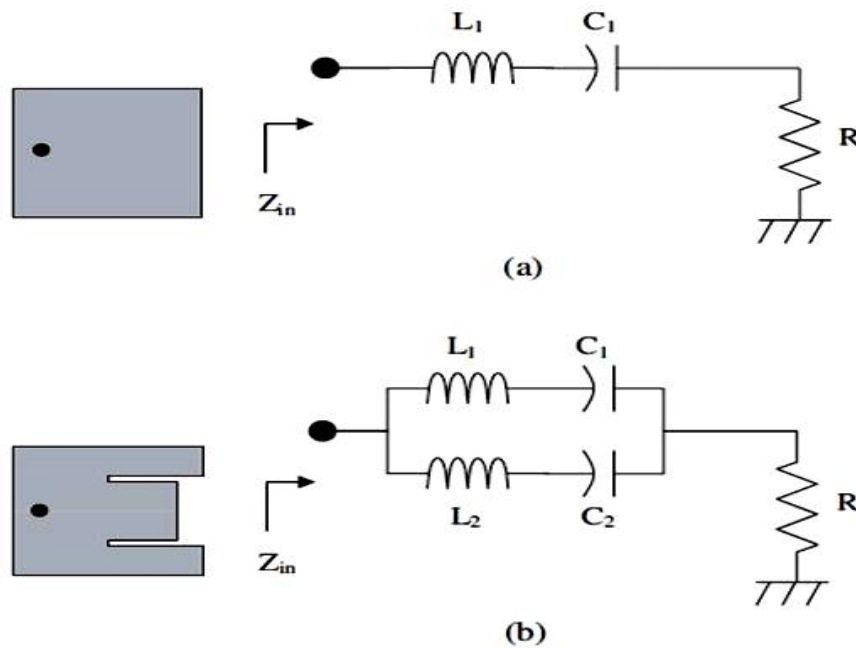


Figure 2.10: Equivalent circuits of (a) Rectangular Patch and (b) E shaped Microstrip Antennas.

A common rectangular patch antenna can be represented by means of the equivalent circuit of Figure 2.10 (a). The resonant frequency is determined by L_1C_1 . At the resonant frequency, the impedance of the series LC circuit is zero, and the antenna input impedance is given by resistance R . By varying the feed location, the value of resistance R may be controlled such that it matches the characteristic impedance of the coaxial feed, usually the input impedance is match at 50Ω . When a pair of slots is incorporated, the equivalent circuit can be modified into the form as shown in Figure 2.10 (b).

The second resonant frequency is determined by L_2C_2 . Analysis of the circuit network shows that the antenna input impedance is given by –

$$Z_{in} = R + j \frac{(\omega L_1 - 1/\omega C_1)(\omega L_2 - 1/\omega C_2)}{\omega(L_1 + L_2) - (1/\omega C_1 + 1/\omega C_2)}$$

The imaginary part of the input impedance is zero at the two series resonant frequencies determined by L_1C_1 and L_2C_2 , respectively. Of course, this is by no means the exact model of the E-shaped antenna because the equation shows that there is a parallel-resonant mode between the two series-resonant frequencies. Nevertheless, it serves to explain the operating principle of the antenna design. If the two series resonant frequencies are too far apart, the reactance of the antenna at the midband frequency may be too high and the reflection coefficient at the antenna input may be unsatisfactory. If the two series-resonant frequencies are set too near to each other, the parallel-resonant mode may affect the overall frequency response and the reflection coefficient near each of the series-resonant frequencies may be degraded. The question now is: how would the slot length, slot width, slot position and the length of center arm affect the values of L_2 and C_2 . This patch shape has shown to enhance gain as well as bandwidth of microstrip patch antenna. E-shaped patch antenna is much simpler in construction. By only adjusting the length, width, and position of the slots, we can obtain satisfactory performances. In the E shaped antenna, the amplitudes of currents around the slots are different at low resonant frequencies and high resonant frequencies. It means that the effects of the slots at these two resonant frequencies are different. This is the key reason why the slots can extend the bandwidth. At the high frequency, the amplitudes of the currents around the slots are almost the same as those at the left and right edges of the patch. That means effect of the slots are not significant in high frequencies and the patch works like ordinary patch. Therefore, the high resonant frequency is mainly determined by the patch width, less affected by the slots. While at the low frequency, the amplitudes of the currents around slots are greater than those at high frequency. The slots assemble the currents and this effect can be modeled as an inductance. Due to this additional inductance effect, it resonates at a low frequency. Because of the dual resonant character, this kind of microstrip antenna can achieve a wide bandwidth [1, 2, 3].

An E shaped patch antenna is designed to cover frequency band of 2.34-2.57 GHz having a size of $76 \times 45 \text{ mm}^2$. Although the antenna is for lower frequency range but it provides us with a good insight of the E shaped patch antenna. The antenna is a modified form of the conventional E-shaped patch. By letting the two parallel slots of the E patch be unequal, asymmetry is introduced. This leads to two orthogonal currents on the patch and, hence, circularly polarized fields are excited. The proposed technique exhibits the advantage of the simplicity of the E-shaped patch design, which requires only the slot lengths, widths, and position parameters to be determined. Investigations of the effect of various dimensions of the antenna have been carried out via parametric analysis. Based on these investigations, a design procedure for a circularly polarized E-shaped patch was developed [9].

In [6] researchers designed another E shaped microstrip patch antenna for IEEE 802.11b standard. The wide-band mechanism of this antenna is explored by investigating the behavior of the currents on the patch. The slot length, width, and position are optimized to achieve a wide bandwidth. Finally, E-shaped patch antenna, resonating at wireless communication frequencies of 1.9 and 2.4 GHz, is designed, fabricated, and measured. The radiation pattern and directivity are also presented. This antenna dimension was in scale of $70 \times 50 \text{ mm}^2$.

In 2008 M A Matin and M A Mohd Ali demonstrated a low cost, compact stacked E-shaped patch antenna. The simulation results of its performance are investigated and the return loss is found under -10 dB for the band 3.1-4.9 GHz, which is better than the square patch stacked E-shape patch antenna. The dimension and position of the rectangular patch as well as the shift of coaxial probe location have been optimized to achieve this wide bandwidth and it can be used for UWB lower band applications. This antenna has double substrate layer resulting a total height of 11.6 mm. Size of the antenna is $37.4 \times 31.7 \text{ mm}^2$ [21].

Another patch antenna with a slot and a tuning stub, or called a Modified E-shaped Patch (ESP), has been studied in [8]. Simulation has shown that the tuning stub has introduced a new resonant frequency, resulting in a bandwidth of 380 MHz (5.3-5.75 GHz) with a central frequency of 5.58 GHz while the bandwidth of a

common rectangular patch of the same size on the same substrate is 220 MHz by simulation and 254 MHz by experiment.

In [7] a very good antenna having a size of 33.2x22.2 mm² is described. Theoretical analyses and preliminary experiments indicate that these antennas have a return loss > 10 dB in the two IEEE 802.11a wireless bands, namely 5.15-5.35 GHz and 5.725-5.825 GHz. This antenna can cover USA and European standard of WLAN, where this thesis targets a higher frequency band that covers all the standards in between 4.9 GHz to 5.825 GHz.

Another antenna covering two different bands resonating at 5.3 GHz and 7.4 GHz is designed in [22] with impedance bandwidth of 760.43 MHz and 1.39 GHz respectively. Slots in the ground plane and multiple element arrays are used to achieve better bandwidth. The antenna can be used for high speed (IEEE 802.11a) wireless computer local area network (WLAN) and other wireless application.

CHAPTER 3

PROPOSED ANTENNA

3.1 Specifications

Our primary objective is to design an antenna that can serve all the hi-speed WLAN standards available throughout the world in the 5-6 GHz ranges. More specifically our antenna should support:

- 802.11a (USA) or 5.15-5.35 GHz band;
- European 802.11a or 5.725-5.825 GHz band;
- Middle-eastern WLAN or 5.47–5.825 GHz band;
- Newly approved IEEE 802.11j or 4.9-5.1 GHz band;

So overall my proposed design should provide at least -10 dB return loss for the total band of 4.90-5.825 GHz. Actually the bandwidth of the antenna can be said to be those range of frequencies over which the RL is less than -9.5 dB (-9.5 dB corresponds to a VSWR of 2 which is an acceptable figure). But to be on the safe side here -10 dB return loss is taken as acceptable. Recent works on the E shaped patch antenna shows us that antenna dimensions for 5-6 GHz band was limited by $33.2 \times 22.2 \text{ mm}^2$. The optimized antenna should have smaller dimensions.

Expression for resonance frequency of an E-shaped microstrip antenna has been found in [23]. Here the resonance frequencies are calculated by equating its area to an equivalent area of a rectangular microstrip patch antenna. A expression for effective dielectric constant is given for the E-shaped microstrip patch antenna. The new expression of resonance frequencies showed a good agreement with measured result. Here in this thesis those expressions are used to find out different dimensions of the E shape patch antenna for lower resonance frequency of 4.95 GHz and higher resonance frequency of 5.77 GHz. Substrate dielectric constant is chosen as 2.2 and height as 5 mm. Parameters found from the calculation are: $W = 33.89 \text{ mm}$, $L = 18.69 \text{ mm}$, $W1 = 10.45 \text{ mm}$, $W2 = 8.87 \text{ mm}$, $L1 = 12.66 \text{ mm}$ and $Ls =$

13.81 mm. As a starting reference we are going to use these parameters to design a simplest form of the E shape antenna. Then optimization is done by changing several parameters to find out the most suitable antenna for our particular operation. To observe the the resonance condition, return loss S_{11} parameter is taken into account. After finding out the parameters which can produce an acceptable return loss response for 4.9-5.82 GHz range, we proceed to observe radiation pattern and current distribution of the found antenna at different operating frequency.

3.2 Optimization

As stated earlier antenna dimensions have been found using empirical expressions from [23]. To keep the design simple the parameters are rounded up to the nearest integers. So the antenna dimensions are $W = 34$ mm, $L = 19$ mm, $W1 = 10$ mm, $W2 = 9$ mm, $L1 = 13$ mm and $Ls = 13.8$ mm. Substrate Dielectric Constant, $\epsilon_r = 2.2$ and $H = 5$ mm. Now a single antenna with these dimensions is designed and simulated using IE3D.

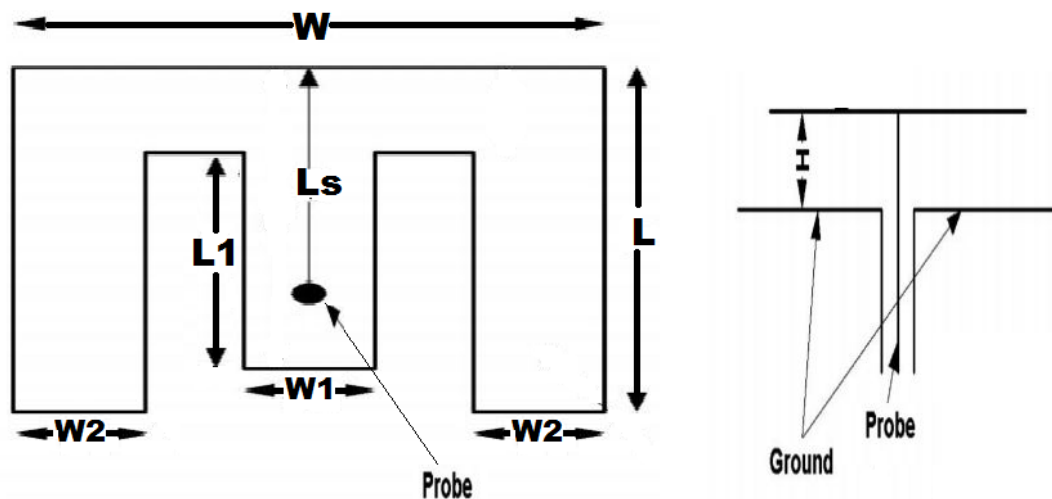


Figure 3.1: Primary Antenna

Return loss of the designed antenna shows us a resonant condition at 4.9 GHz. This is due to the anomaly in the expressions used in the calculation. Those expressions were optimized for E shape patch antenna for lower frequency band of

2-3 GHz band. Although resonance frequency of this antenna is not what we desire, but as a starting reference point this antenna is good enough for parametric analysis in order to optimize the antenna into our desired frequency band of 4.9 GHz to 5.82 GHz.

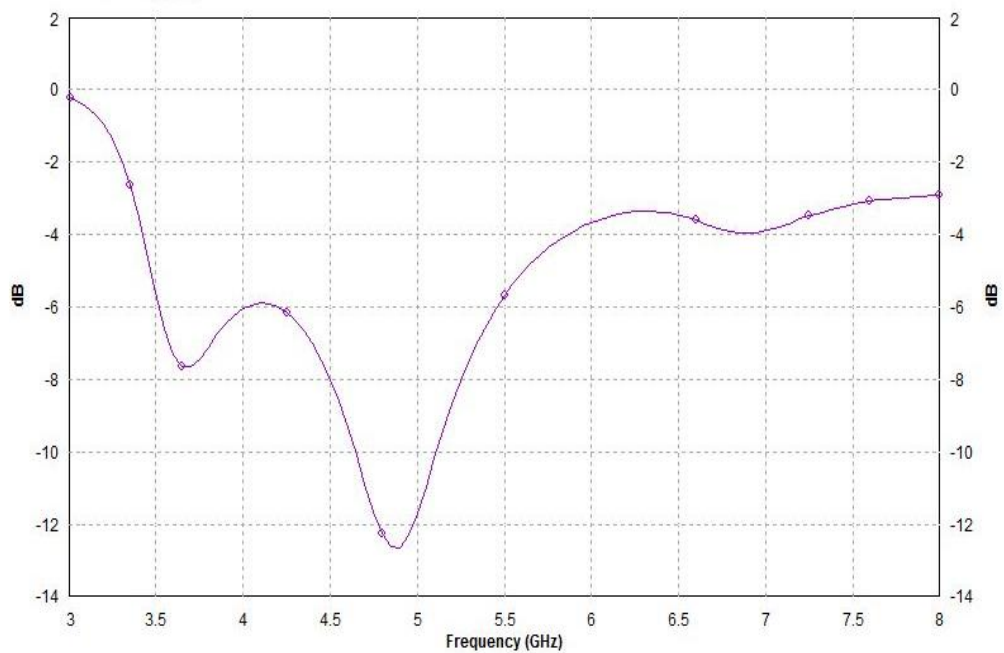


Figure 3.2: Return loss of the primary antenna

Now we are going to observe and comment on the return loss found for the change of the antenna parameters W , L , L_1 , W_1 and L_s . First W is changed to higher value.

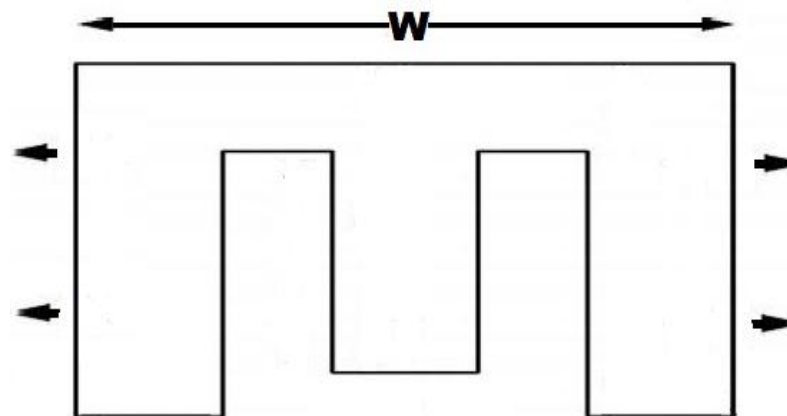


Figure 3.3: Increasing W

The width W is increased from 34 mm to 36 mm and 38 mm to see the effect on the frequency response.

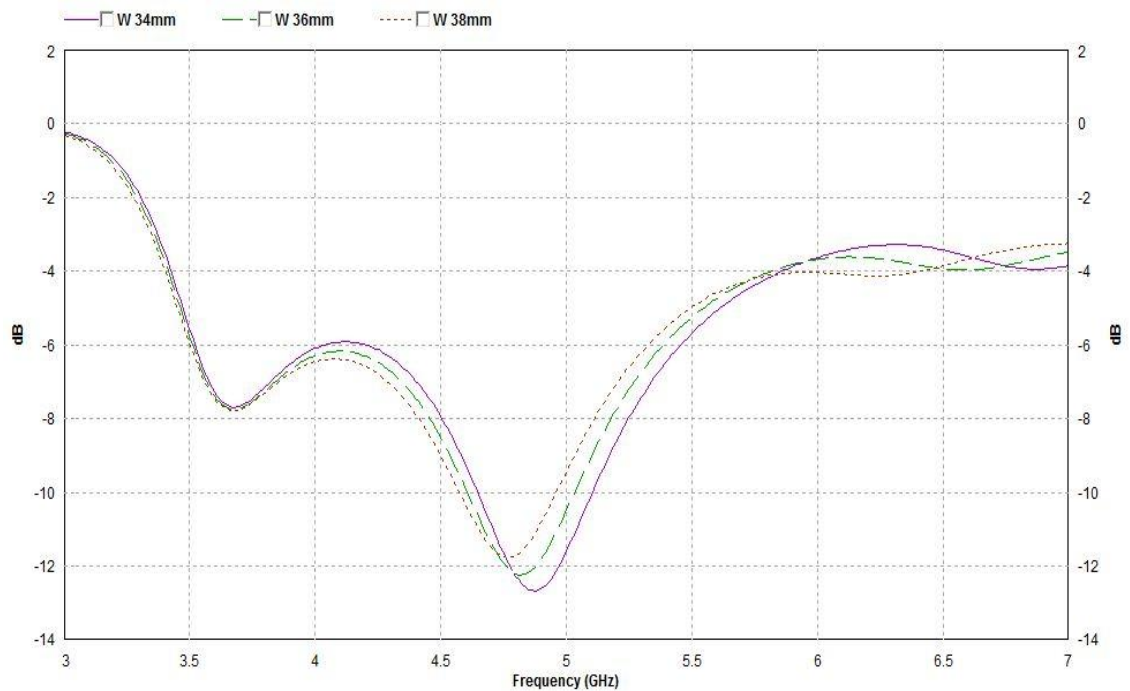


Figure 3.4: Frequency Response for $W = 34, 36, 38$ (mm)

As the W is increased from 34 mm, the resonant frequency shifting to its left and the return loss is also degrading. Both them are unwanted scenarios. So now we should decrease W from 34 so that resonant frequency shifts to its right until return loss reaches its lowest possible value.

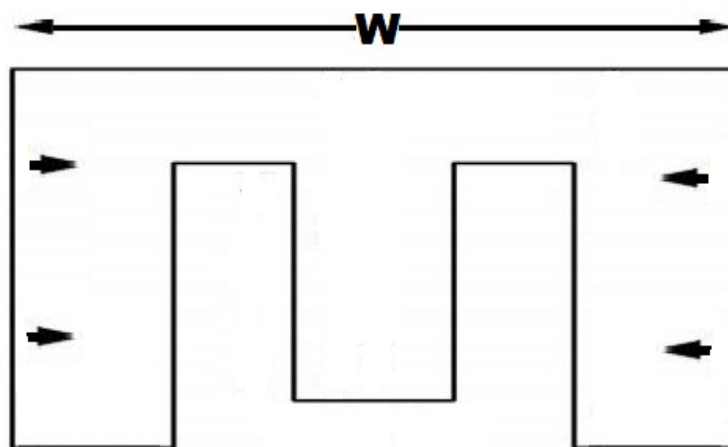


Figure 3.5: Decreasing W

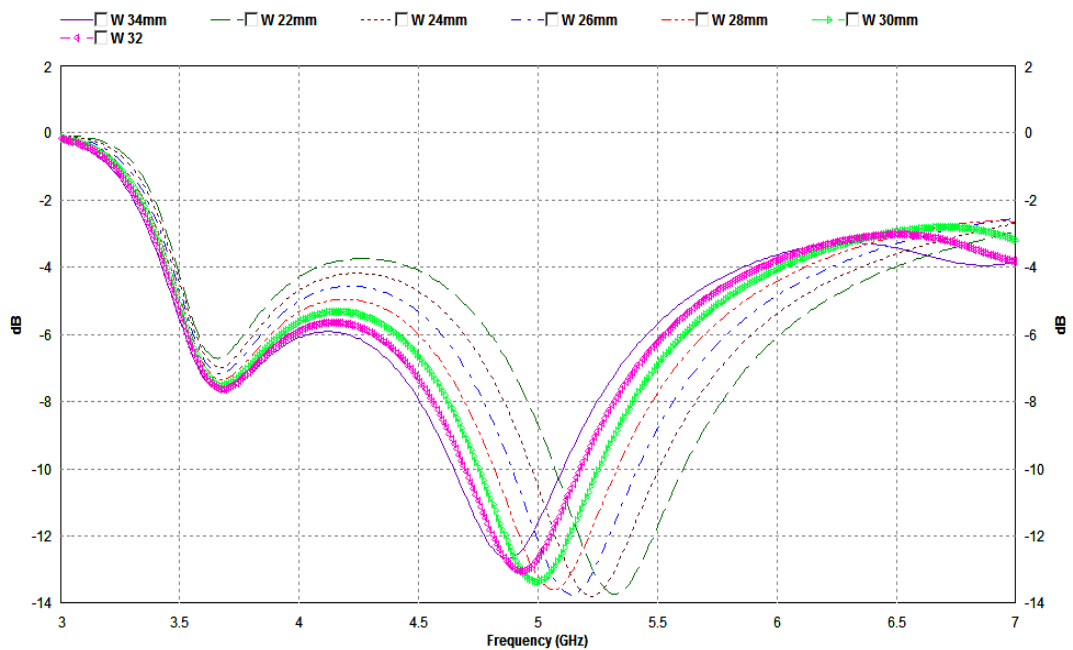


Figure 3.6: Frequency Response for $W = 34, 32, 30, 28, 26, 24, 22$ (mm)

So from Figure 3.6 we can see as we were decreasing the value of W , the RL improves until $W = 26$ mm. For $W = 26$ mm, 24 mm RL are almost equal, whereas at $W = 22$ mm it starts increasing which is unwanted. Again at $W = 26$ mm, -10 dB return loss covers 4.89-5.416 GHz where for $W = 24$ mm, -10 dB RL crosses our lower limit of 4.9 GHz. So now W is fixed at 26 mm.

Next set of simulations are done with the width of the middle arm $W1$. In original antenna $W1 = 10$ mm. Now let's observe the frequency response for $W1 = 12$ mm.

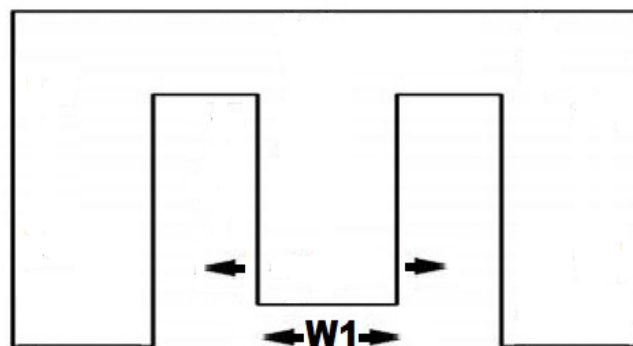


Figure 3.7: Increasing $W1$

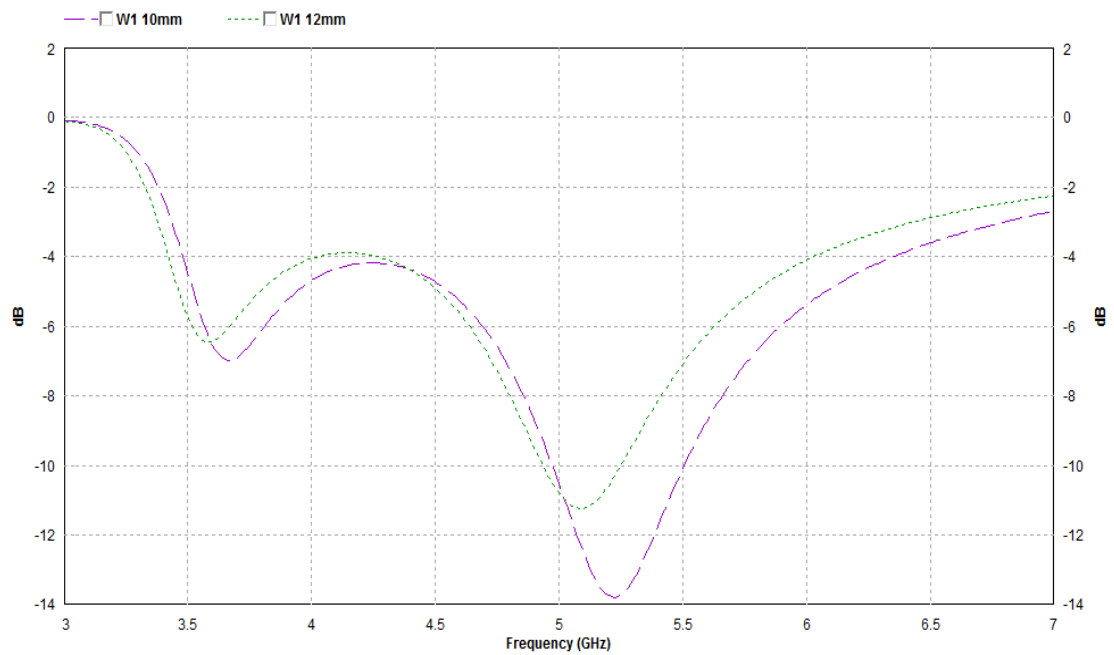


Figure 3.8: Frequency Response for $W1 = 10, 12$ (mm)

So increased $W1$ is degrading our frequency response. Now we should decrease $W1$ to make response better. Figure 3.10 shows the frequency response of the antenna for $W1 = 10$ mm, 8 mm, 6 mm, 5 mm and 4 mm. Decreasing $W1$ from 10 mm to 4 mm widens the bandwidth more and more, but at $W1 = 4$ mm the response curve moves far right than our desired band. So $W1 = 5$ mm provides the best return loss of -44 dB at 5.54 GHz with higher than -10 dB return loss for frequency range of 5.12-6.01 GHz.

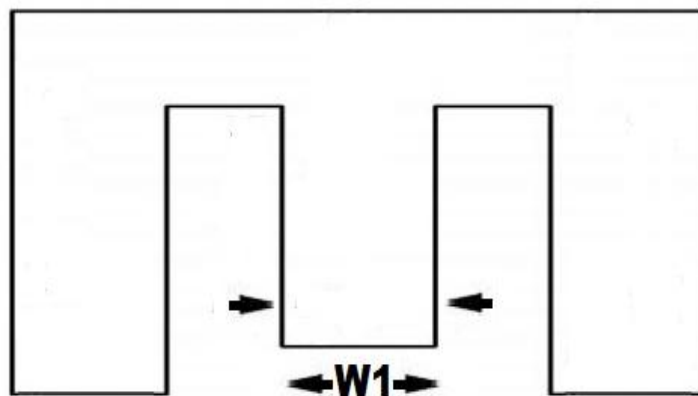


Figure 3.9: Decreasing $W1$

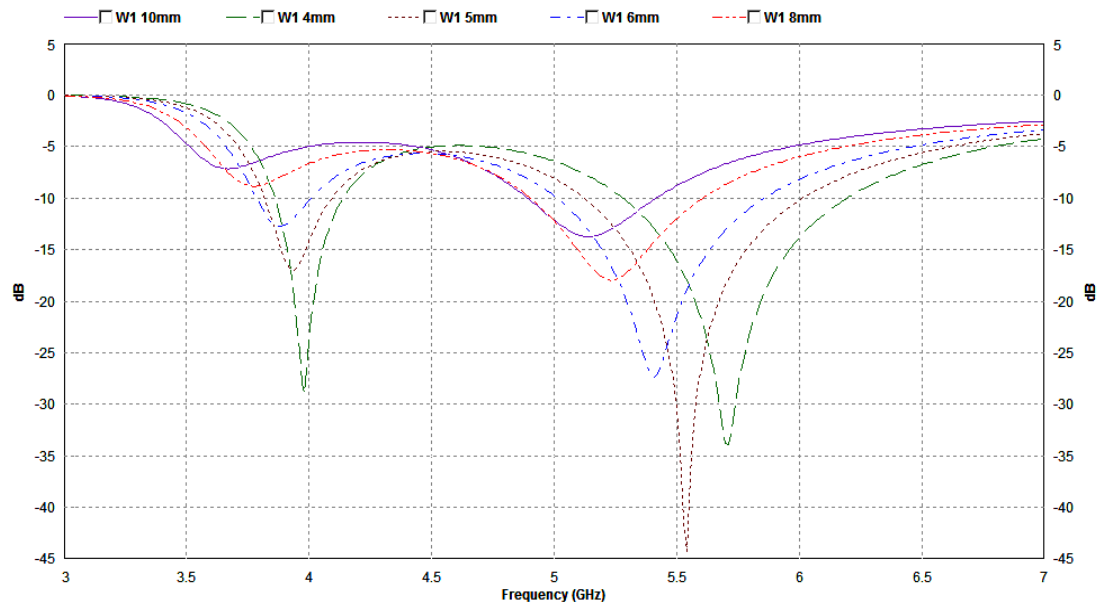


Figure 3.10: Frequency Response for $W1 = 10, 8, 6, 5, 4$ (mm)

So for the next phase we proceed with $W1 = 5$ mm. Now we are going to change length L to see its effect on frequency response. At first L is changed by moving the top boundary up and down by 1 mm.

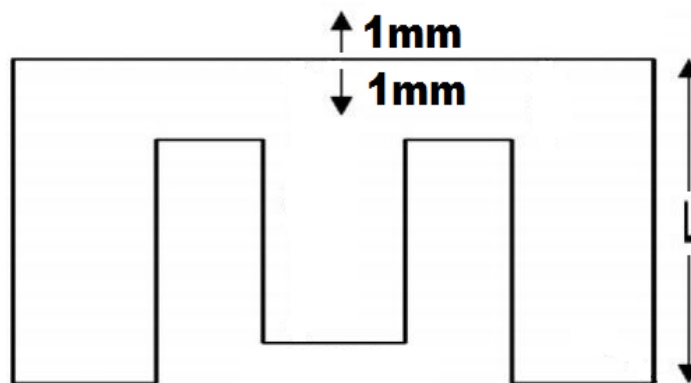


Figure 3.11: Changing L from the top

From Figure 3.12 we observe that both increasing and decreasing of L from the top side results in more return loss and lower bandwidth. So we can go back to $L = 19$ mm. Now L can be changed from the downside to observe its effect on bandwidth and return loss. It should also be noted that increasing L from top moves the curves leftwards and decreasing L moves the curves in opposite direction.

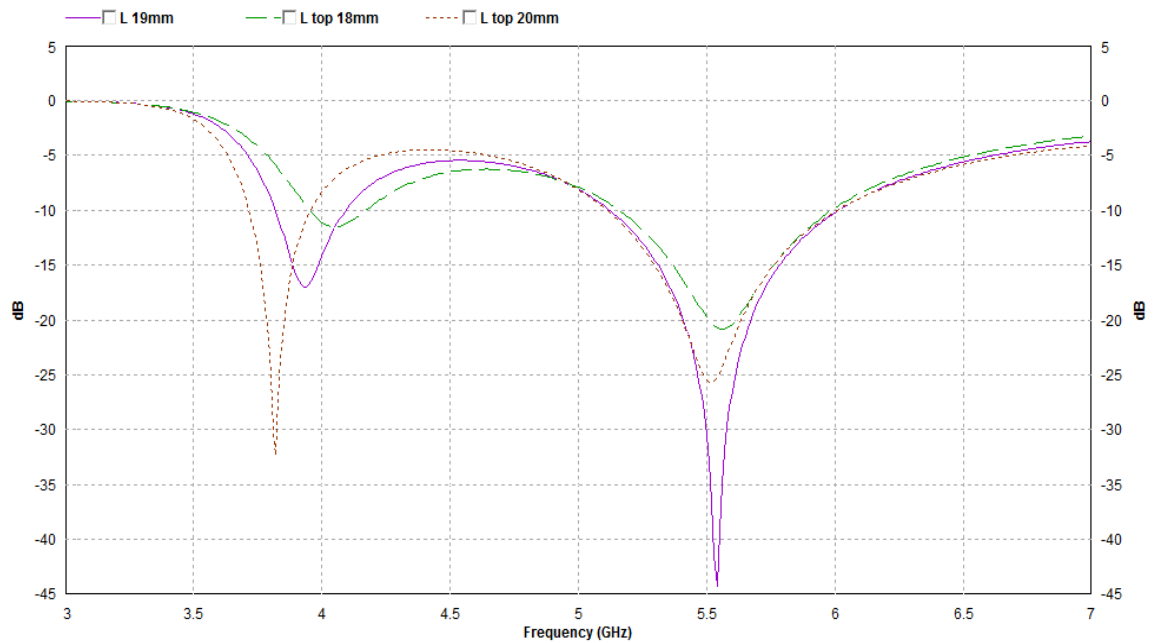


Figure 3.12: Frequency Response for $L = 19, 18, 20$ (mm)

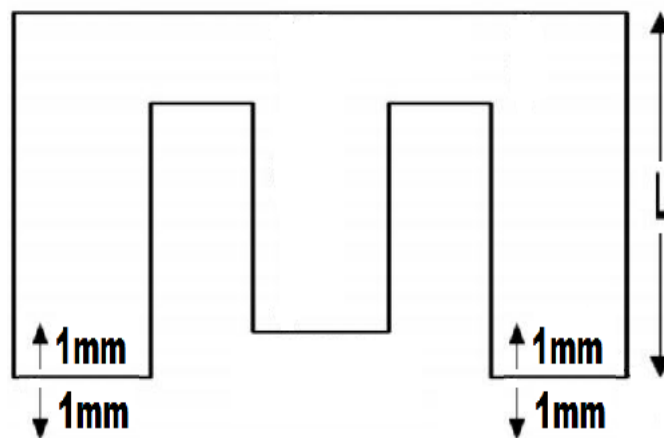


Figure 3.13: Changing L from the bottom

Figure 3.14 shows us that changing L from the bottom also degrades our frequency response by increasing return loss. And again loss just like the previous case decreasing L from top moves the curves rightwards and decreasing L moves the curves in opposite direction.

So our length L is now optimized for best output as $L = 19$ mm. Any change of length from 19 mm hampers the RL significantly.

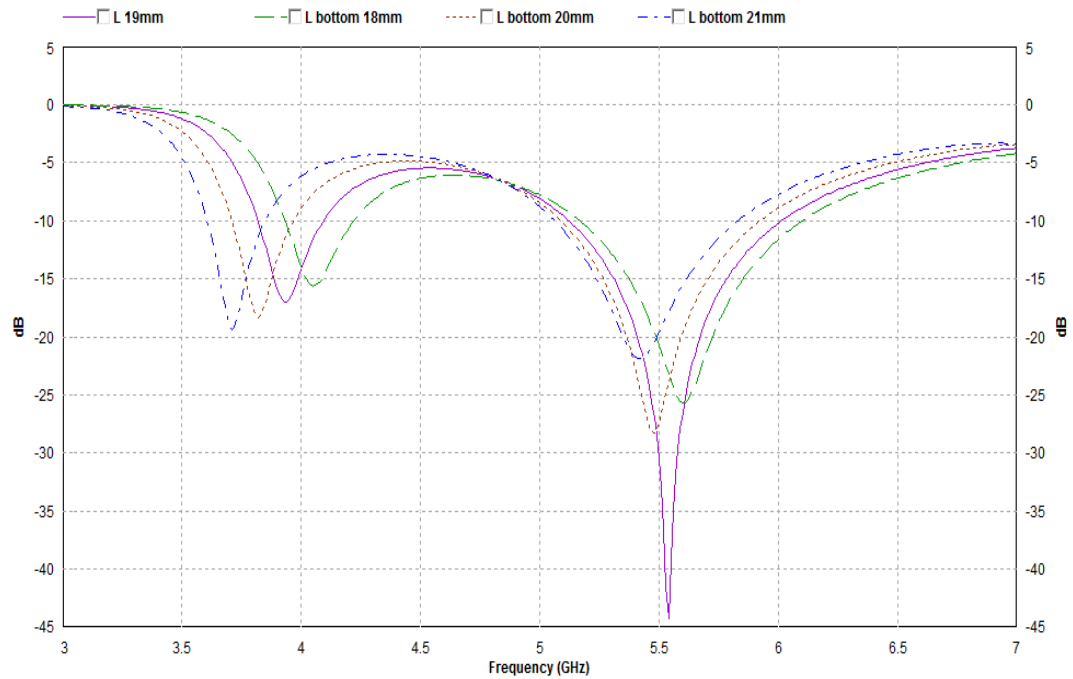


Figure 3.14: Frequency Response for $L = 19, 21, 18, 20$ (mm)

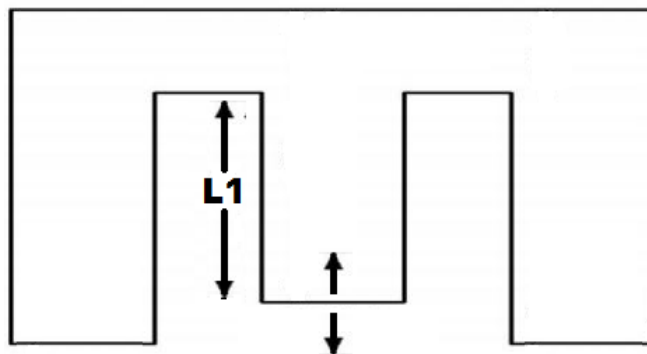


Figure 3.15: Changing $L1$

So far three parameters L , W , $W1$ have been optimized for a frequency range of 5.12 GHz to 6.01 GHz. The primary objective is to get frequency range of 4.9 GHz to 5.825 GHz. Next phase of optimization is done with the non optimized parameter $L1$.

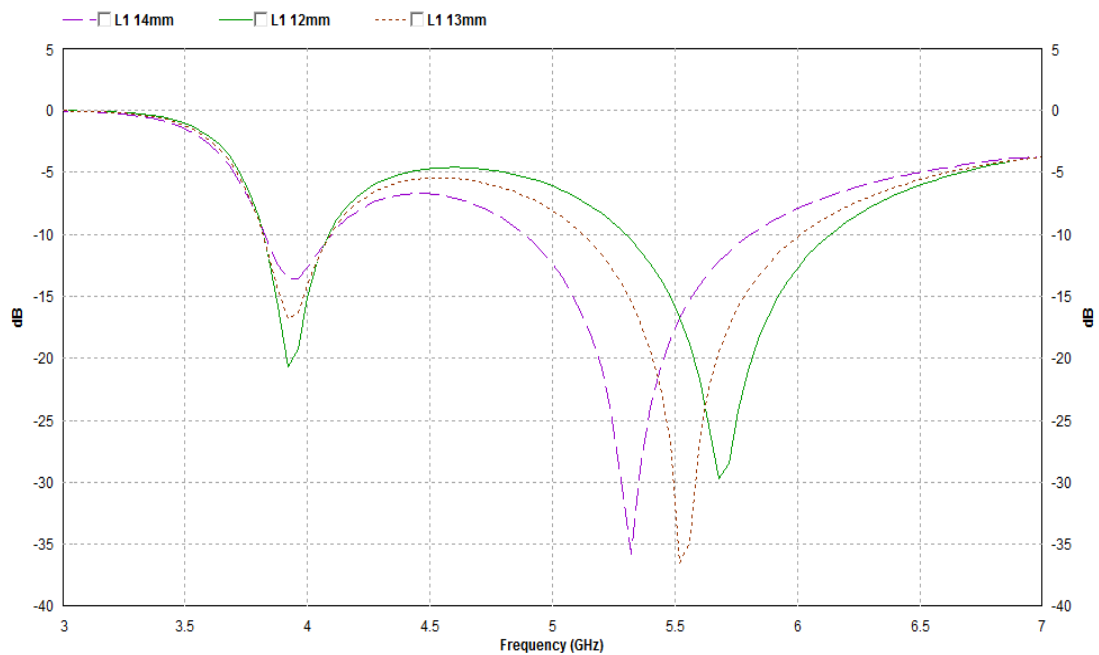


Figure 3.16: Frequency Response for changing L1

So in the Figure 3.16 we can see changing L1 from 13 to 12 increases the return loss and moves the resonant frequency to the right. While increasing L1 from 13 to 14 keeps the RL almost same but moves the resonant frequency to left. At L1 = 14 the frequency range having greater than -10dB return loss becomes 4.88-5.811 GHz which almost covers the desired band.

Next W2 is changed from 9 mm to 8 mm and 10 mm to observe the effect on return loss and bandwidth.

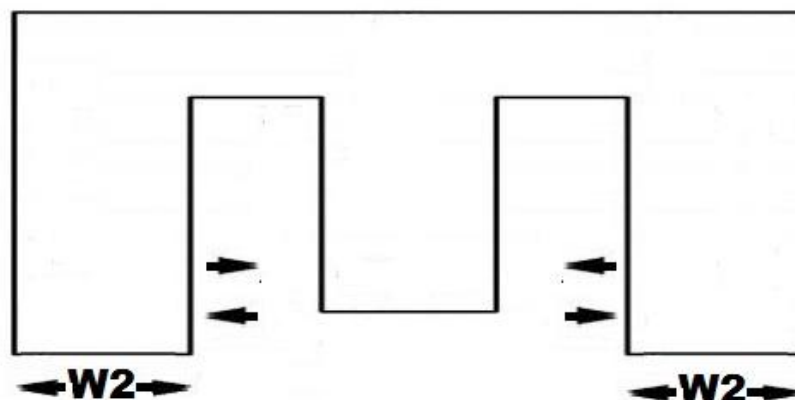


Figure 3.17: Changing W2

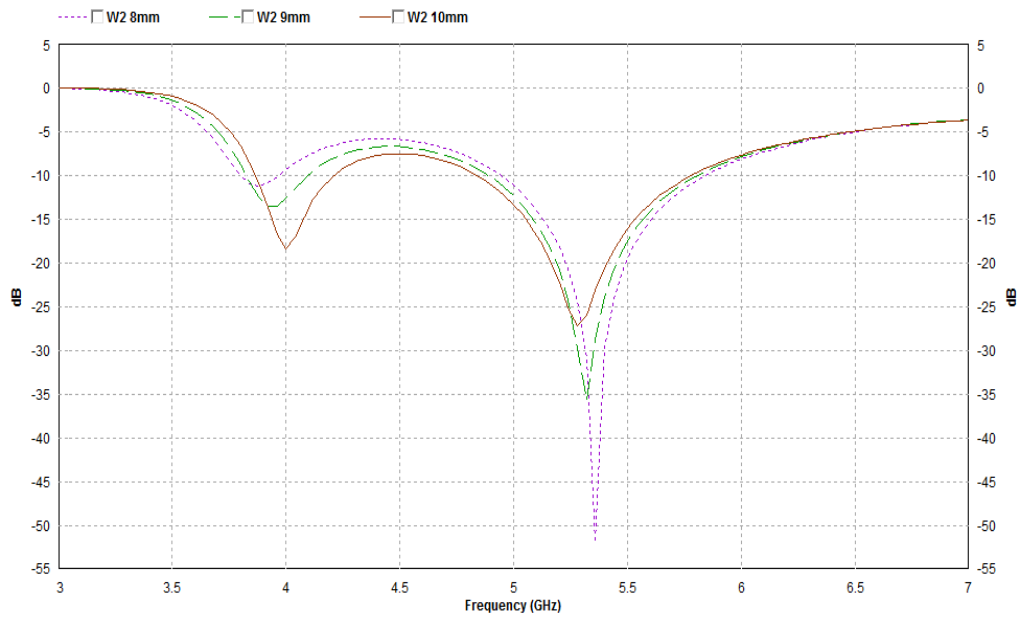


Figure 3.18: Frequency Response for changing W2

So we can see increasing W2 moves the response leftwards and degrades the return loss whereas decreasing W2 moves the response rightward and improves the return loss. But although return loss is lower we cannot take it because the lower -10dB frequency crossing our threshold of 4.9 GHz. So $W2 = 9$ mm is best option.

Ls is last parameter to study. Ls is change from 13.8 mm to 12.8 mm and 14.8 mm. Comparison between their return loss vs frequency curve is shown below.

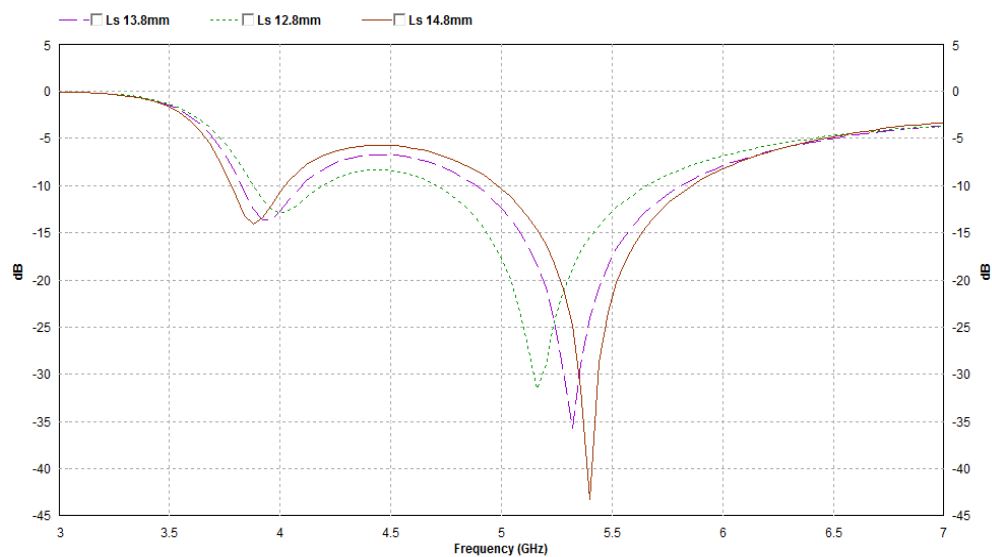


Figure 3.19: Return loss for changing Ls

Changing L_s changing the resonant frequency which is worse than the situation $L_1 = 14$ mm of Figure 3.16. Any change in resonant frequency moves the whole coverage bandwidth with it. So L_s is not changed from 13.8.

Now to satisfy the primary objective many points between $L_1 = 14$ mm and $L_1 = 13.8$ mm were simulated. And finally for $L_1 = 13.94$ mm a frequency response was found where the whole range from 4.8966 GHz to 5.8258 GHz achieved more than -10 dB amplification. So our desired criterion is achieved. And final antenna dimension is $W = 26$ mm, $L = 19$ mm, $W_1 = 5$ mm, $W_2 = 9$ mm, $L_1 = 13.94$ mm and $L_s = 13.8$ mm.

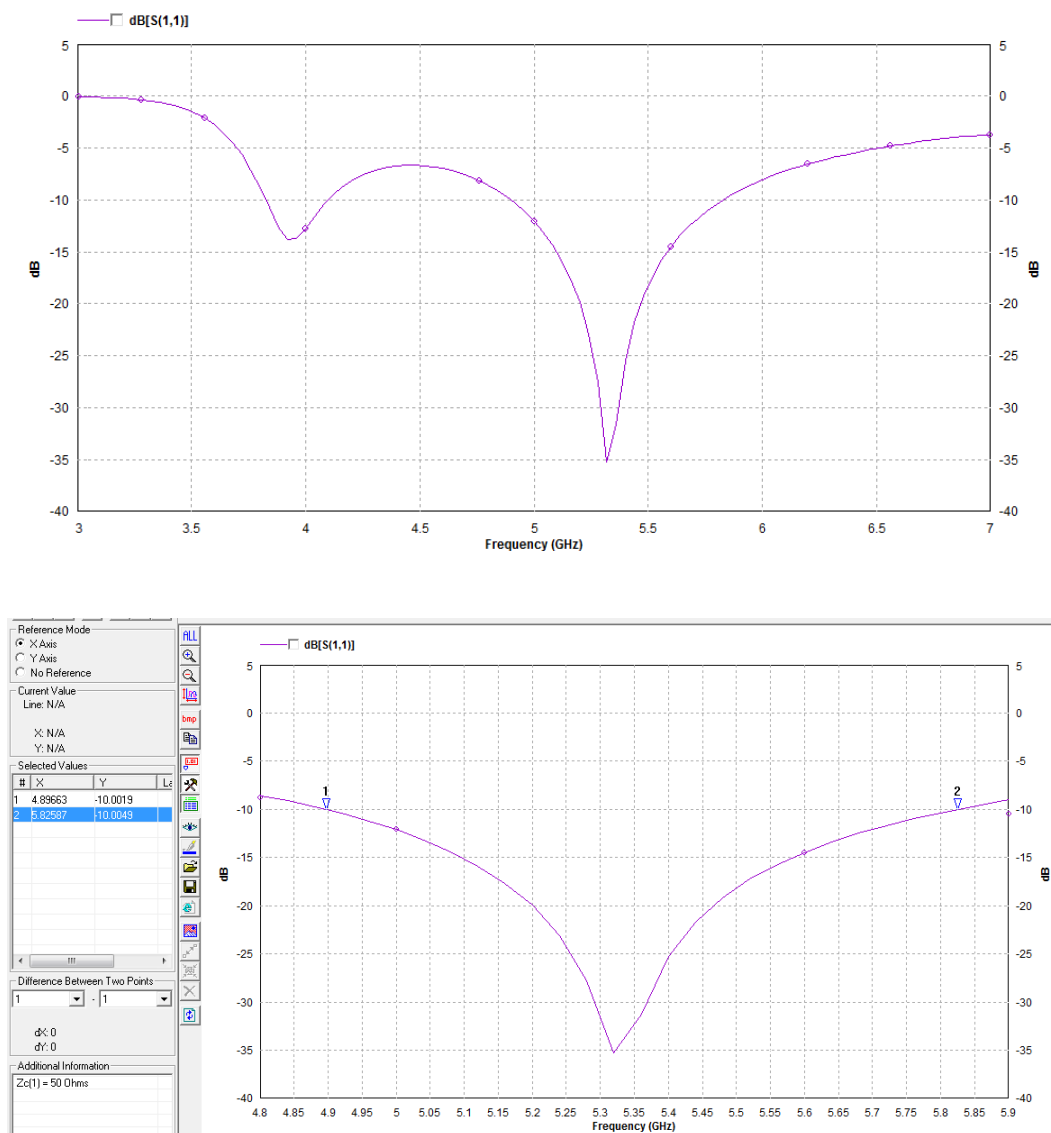


Figure 3.20: Final outcome with desired bandwidth

CHAPTER 4

RESULTS AND SIMULATIONS

In the previous chapter an intensive simulation has been done to optimize the antenna for the frequency range of 4.9-5.825 GHz. As a result we have found an antenna having an area of $26 \times 19 \text{ mm}^2$ with lower than -10 dB return loss for a frequency band of 4.8966 GHz to 5.8258 GHz. Another additional band ranging from 3.8 GHz to 4.1 GHz has also been found under -10 dB return loss which can be very useful for smart devices that use GPS signals from C band satellites. The antenna size is smaller than any of the antenna found in the literature review for the IEEE 802.11a USA and European WLAN standards. Apart from many complex stacked structures for E shape patch antenna a single element single substrate layer antenna has been designed with wide bandwidth. Most of the antenna found in literature review used stacked configuration for substrate layer to enhance the bandwidth and to reduce antenna size. But stacked configuration makes the antenna mechanically vulnerable in some application. The simplicity of designed antenna makes it robust and useful for those operations.

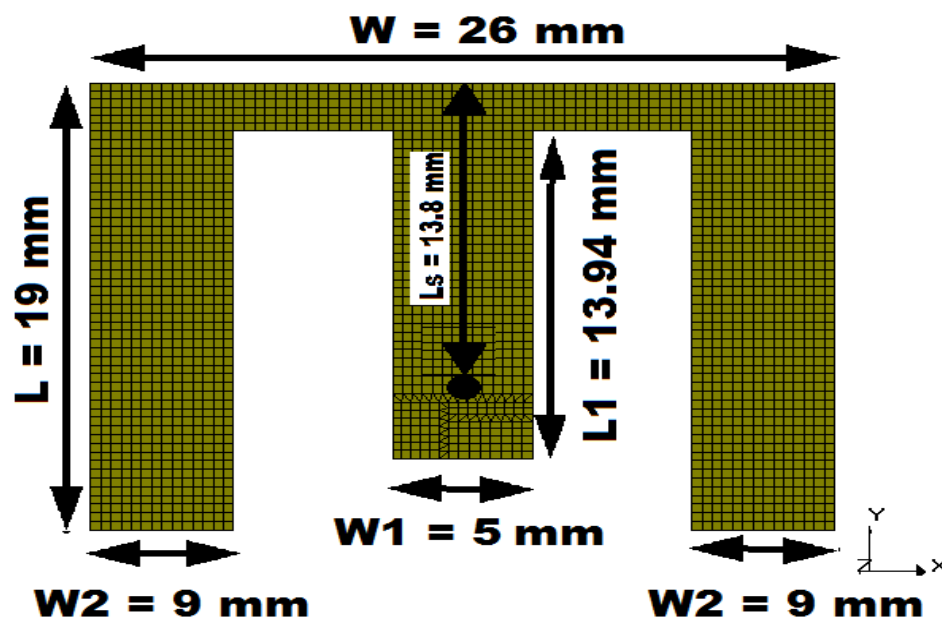


Figure 4.1: Structure view of the final antenna with dimension

Now as our simulated and optimized antenna covers North American WLAN standard ranging from 5.15 to 5.35 GHz, European WLAN standard ranging from 5.725–5.825 GHz, Asian and Middle-eastern WLAN 5.47–5.63 GHz and the newly approved Japanese WLAN standard ranging from 4.9 to 5 GHz frequency bands; we should examine our antenna operation in each of the standards by our antennas average current distribution, vector current distribution, 2D, 3D radiation patterns for a frequency in each bands. The current distribution gives us an insight into the antenna structure by showing the density and the direction of current movement inside the patch at different frequencies. It also gives us how different part of the antenna behaves for different operating frequencies. 2D and 3D radiation pattern shows us how antenna radiates its output signal. 2D radiation profile provides information about the gain and polarization of E-H fields where as 3D radiation patterns can show the directivity and emission style. If all the distribution and pattern at all operating frequencies are found satisfactory only then we can proceed to future works with this simulated model.

For 4.9-5 GHz band, we have calculated the average current distribution, vector current distribution, 2D, 3D radiation patterns for $f = 5$ GHz. For 5.15-5.35 GHz band the average current distribution, vector current distribution, 2D, 3D radiation patterns has been calculated for $f = 5.25$ GHz; $f = 5.5$ GHz has been chosen for 5.47–5.63 GHz. Finally for 5.725-5.825 GHz band 5.775 GHz is chosen for pattern calculations.

4.1 Average Current Distribution

So now we will simulate our antenna four different frequencies $f = 5$ GHz, 5.25 GHz, 5.5 GHz and 5.775 GHz with 70 cells per wavelength for better precision. Then we will observe the average current distribution over the antenna surface.

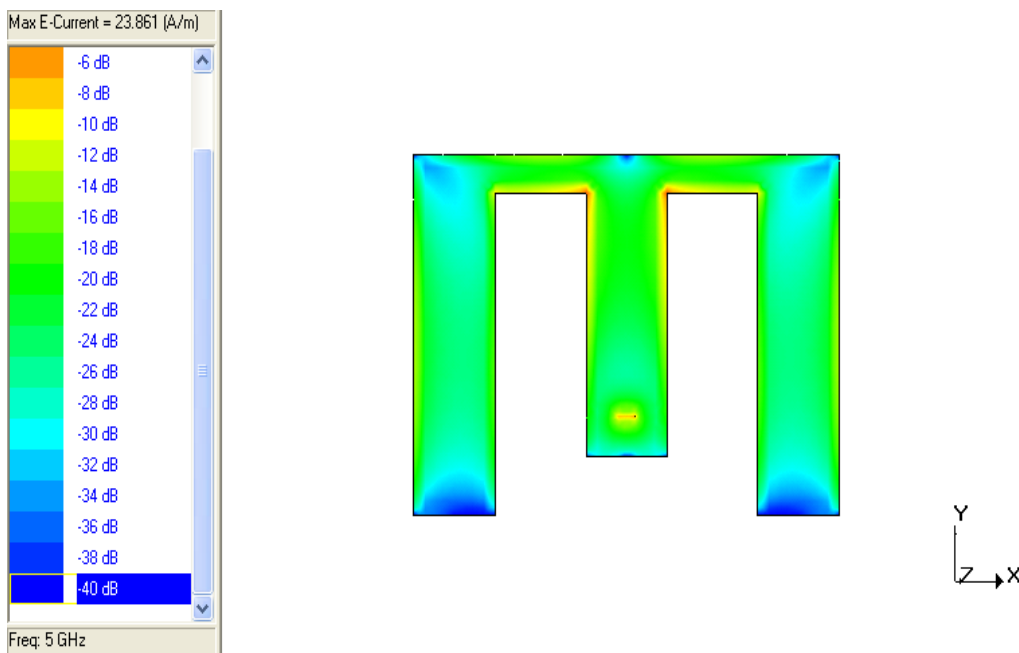


Figure 4.2: Average Distribution of Current 5 GHz

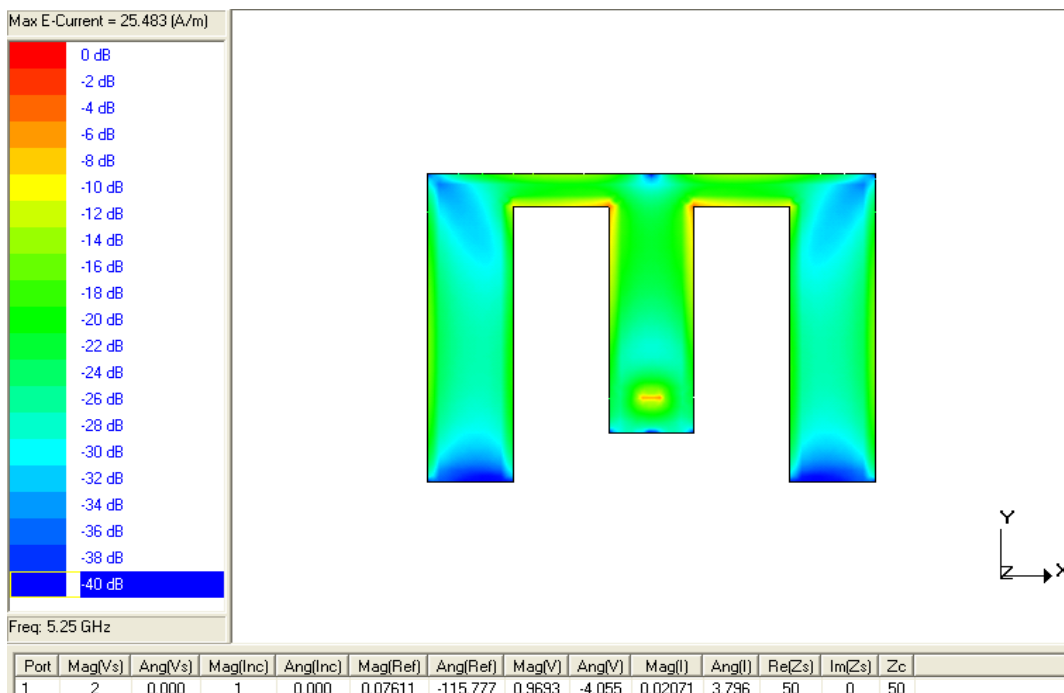


Figure 4.3: Average Distribution of Current 5.25 GHz

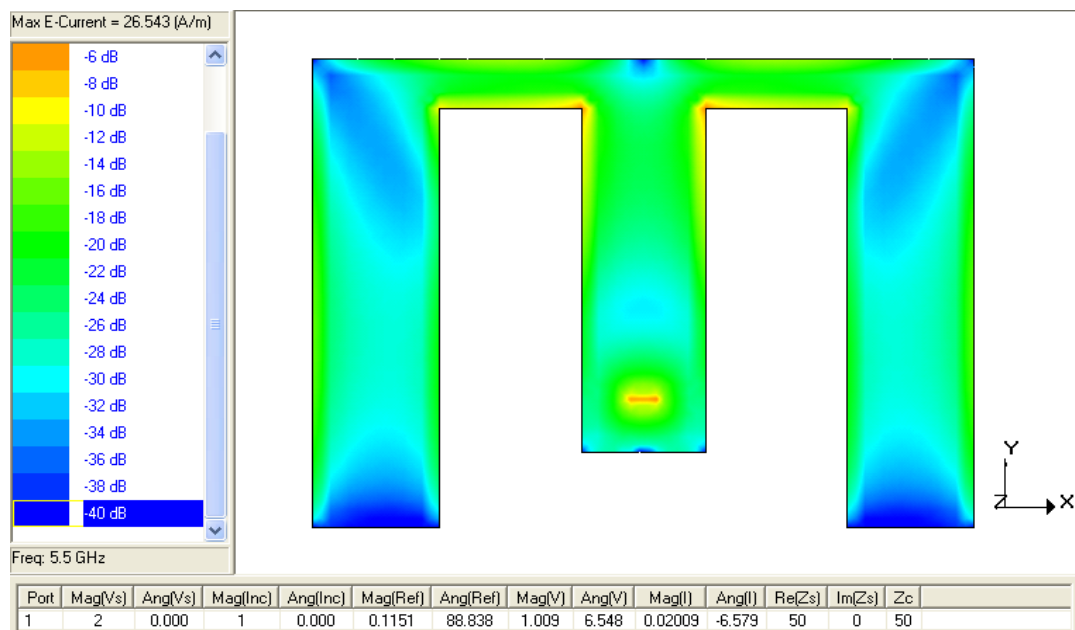


Figure 4.4: Average Distribution of Current 5.5 GHz

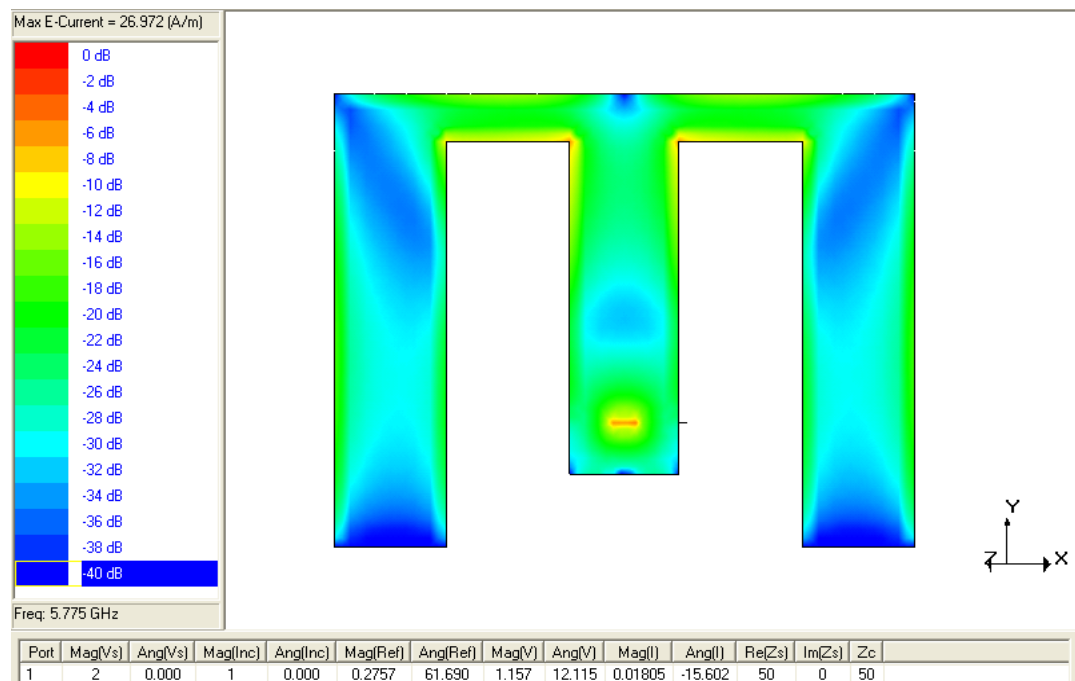


Figure 4.5: Average Distribution of Current 5.775 GHz

Above figures show us the average current distribution over the surface of our optimized patch at different frequencies. For all frequencies current distribution are mostly in green or in blue color corresponding to an amplification of from -20dB to -40dB. Which means for all frequencies in the range of 4.9-5.825 GHz our antenna can work smoothly as a transmitter or a receiver.

4.2 Current Vector Distribution

For same frequencies we will now compare the current vector distribution on the surface of patch to understand the frequency response better. Vector distribution of current can give us insight to the pathway and the movement of current at the resonant frequency over the patch surface. It can also show us the density of current at different frequencies.

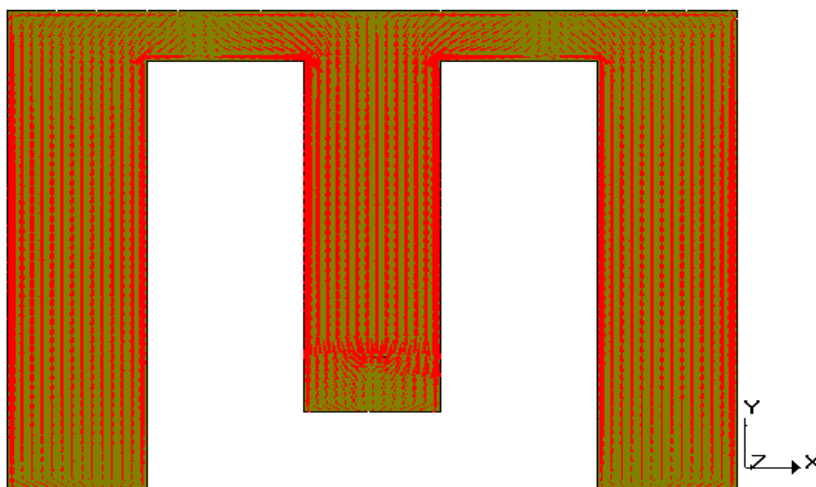


Figure 4.6: Distribution of Current Vectors at 5 GHz

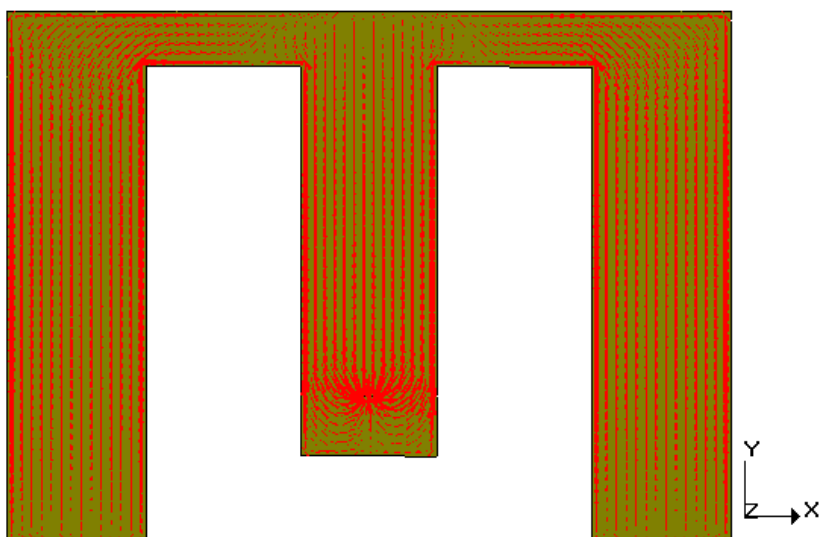


Figure 4.7: Distribution of Current Vectors at 5.25 GHz

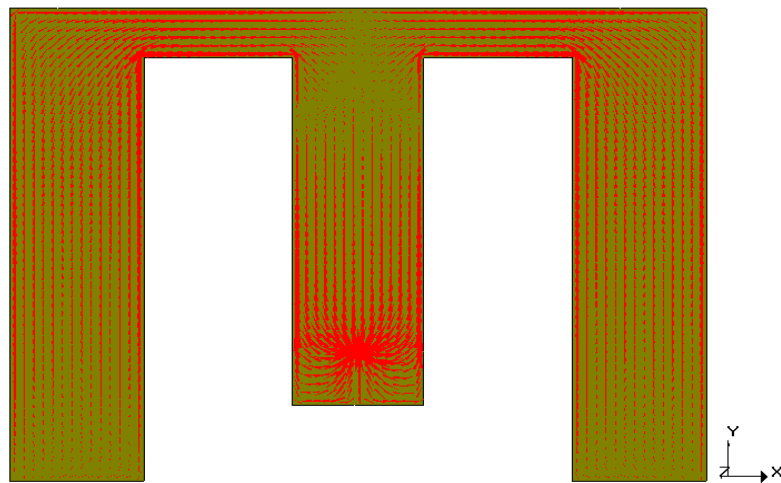


Figure 4.8: Distribution of Current Vectors at 5.5 GHz

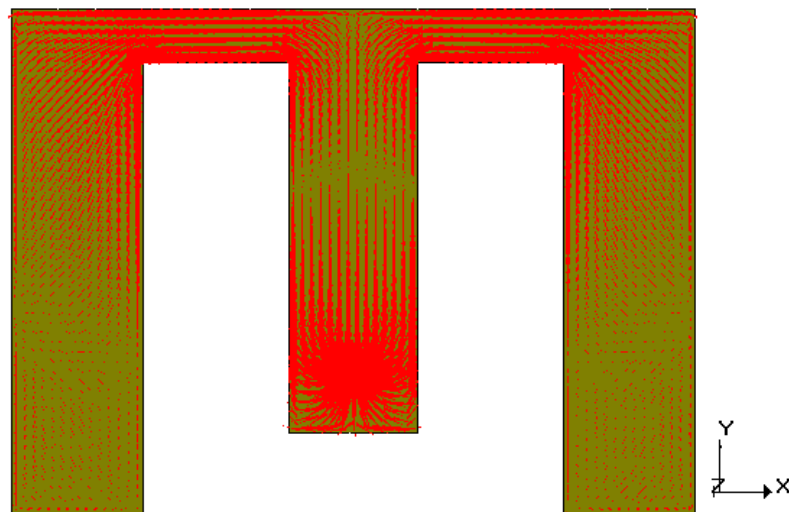


Figure 4.9: Distribution of Current Vectors at 5.775 GHz

The vector distributions of the current over the surface of patch are shown in the above figures. For all four different frequencies current vectors directions are almost similar but in the lower frequencies we can observe the density is higher on the side wings where as in the higher frequencies density is high in the central arm and in the body. But for all frequencies the distribution represents resonant condition which means even in terms of vector distribution our antenna works fine in the WLAN range.

4.3 2D Radiation Pattern

A good antenna should maintain its radiation pattern and polarization throughout the frequency range that it covers. So for our antenna all four frequencies the 2D radiation pattern should be similar to each other.

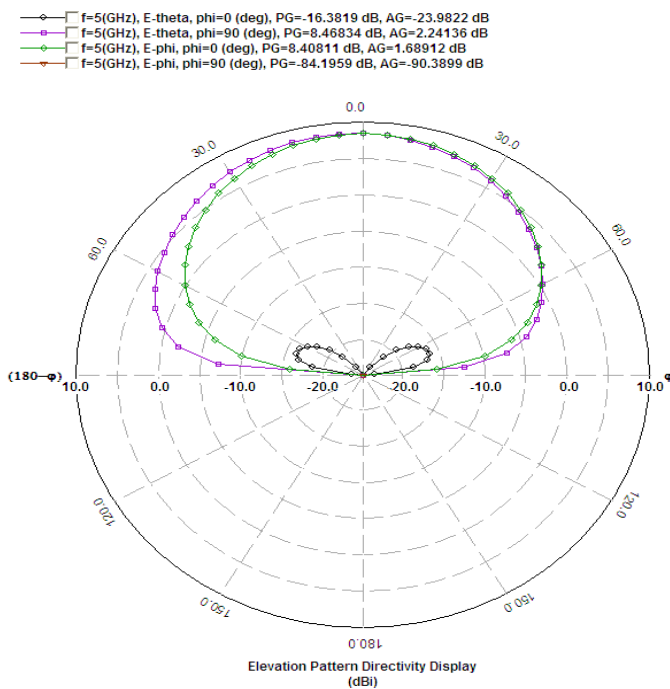


Figure 4.10: 2D Radiation Pattern at 5 GHz

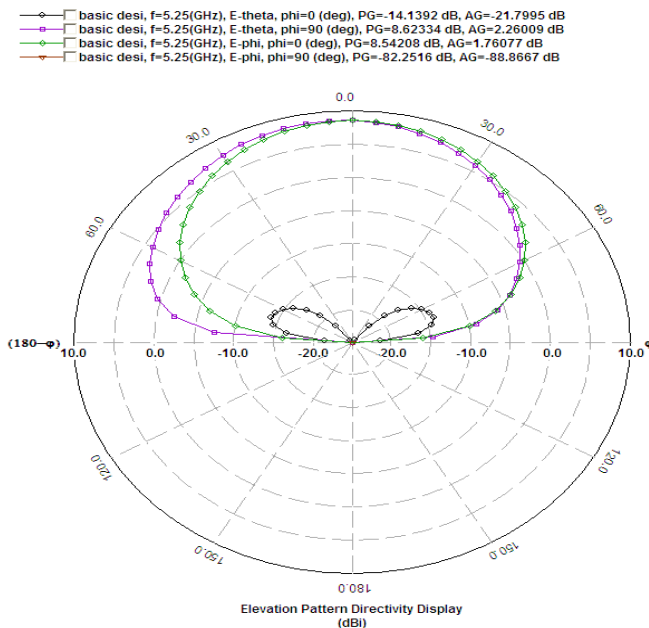


Figure 4.11: 2D Radiation Pattern at 5.25 GHz

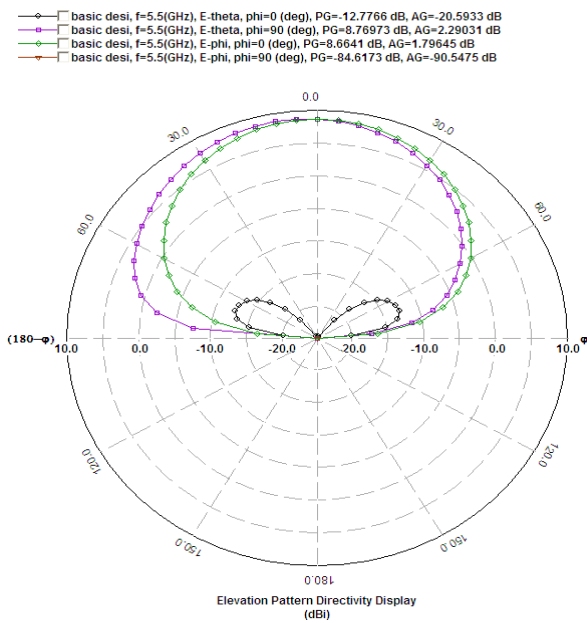


Figure 4.12: 2D Radiation Pattern at 5.5 GHz

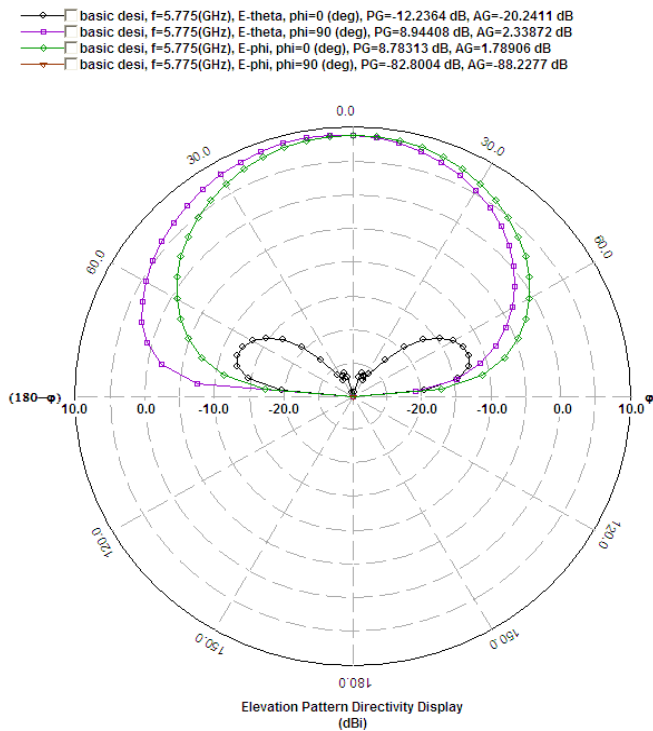


Figure 4.13: 2D Radiation Pattern at 5.775 GHz

2D radiation pattern of all four different frequencies are almost the same indicating that our antenna provides a good radiation pattern and similar polarization for the entire band of 4.9 to 5.825 GHz.

4.4 3D Radiation Pattern

Just like the 2D radiation pattern a good antenna should also maintain its 3D radiation pattern throughout the frequency range that it covers. So for our antenna all four frequencies the 3D radiation pattern should be similar to each other.

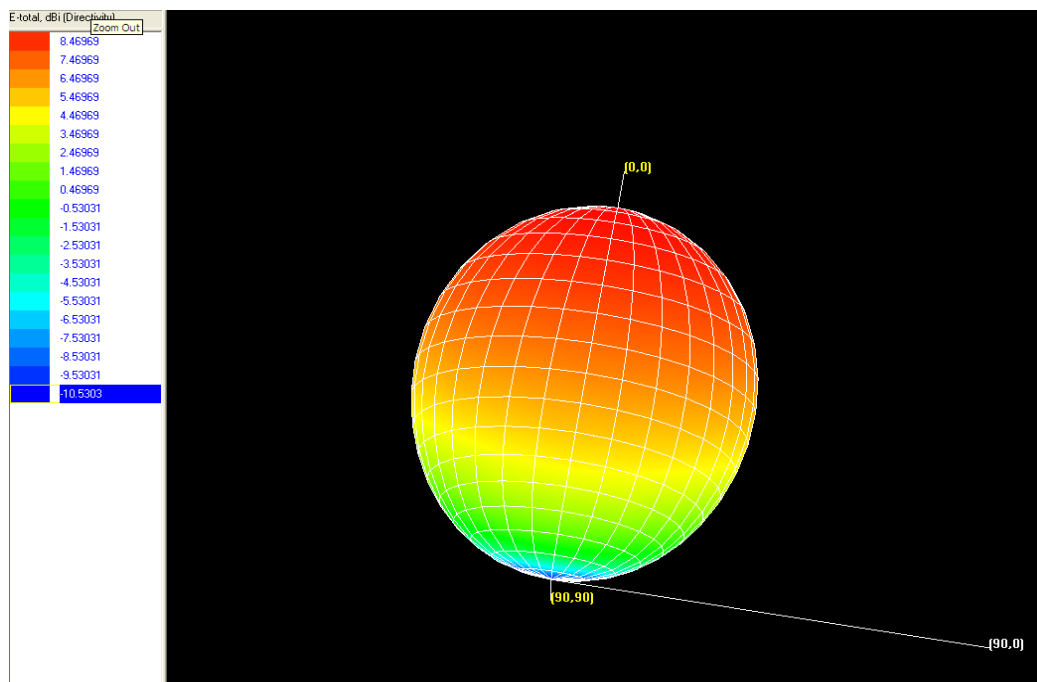


Figure 4.14: 3D radiation pattern at 5 GHz

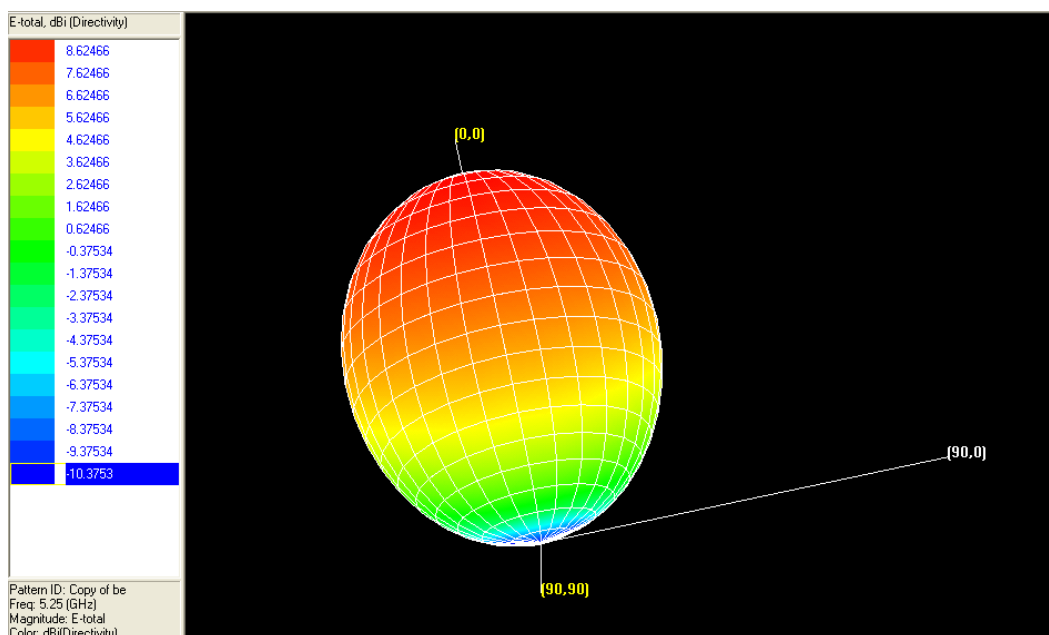


Figure 4.15: 3D radiation pattern at 5.25 GHz

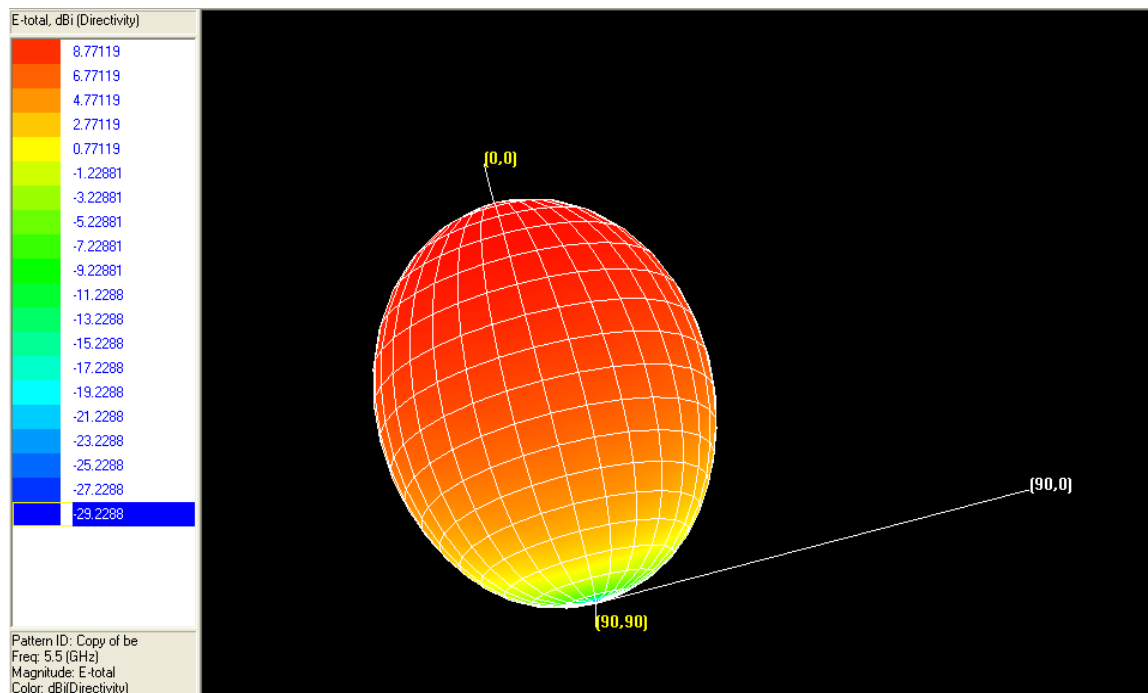


Figure 4.16: 3D radiation pattern at 5.5 GHz

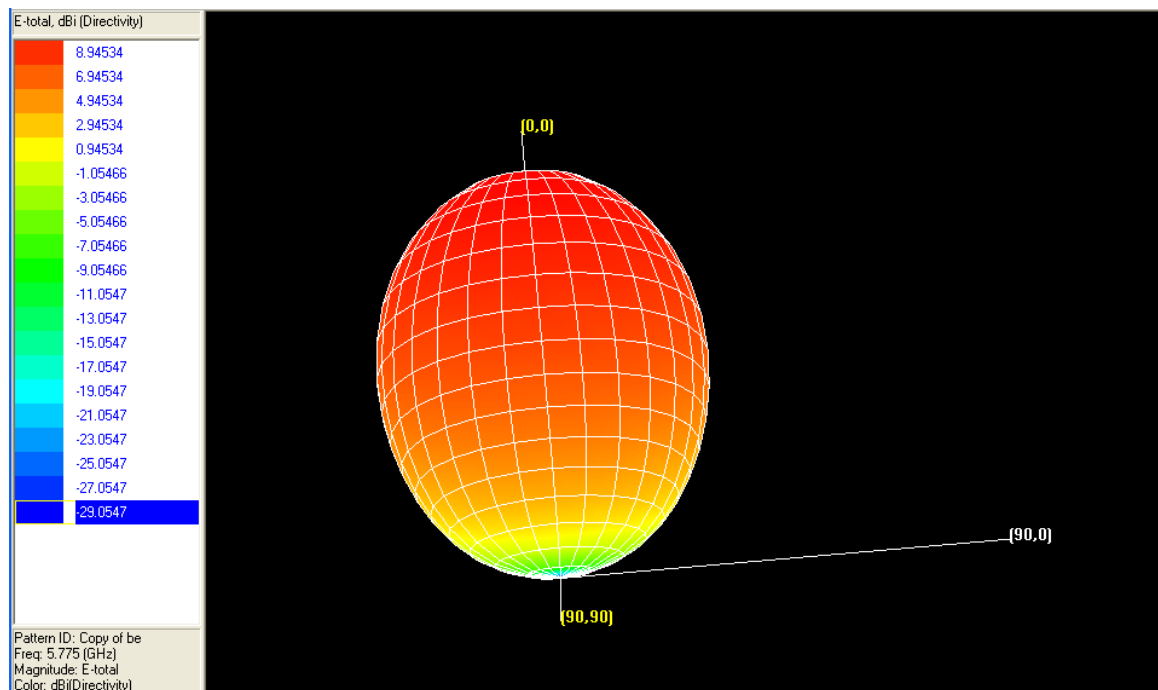


Figure 4.17: 3D radiation pattern at 5.775 GHz

Just like the 2D radiation patterns, 3D radiation profile of our antenna for all four different frequencies are almost the same indicating that our antenna provides a good radiation pattern and similar polarization for the entire band of 4.9 to 5.825 GHz.

4.5 Comparison of the designed antenna with existing antennas

Not much work has been done to design antenna that can operate satisfactorily over all the high speed WLAN standards. In [21], an antenna is designed for 3.1 – 4.9 GHz range covering only a single American special purpose WLAN standard 802.11y where our antenna supports 802.11a, 802.11n, 802.11ac and 802.11j standards. Also our antenna provides a considerable reduction in antenna size and height from [21]. Another E shaped antenna is demonstrated with a bandwidth of 380 MHz with a central frequency of 5.58 GHz [8] where as our antenna provides a huge bandwidth of 925 MHz with frequency band ranging from 4.90 – 5.825 GHz. An antenna to cover two 802.11a standards is designed in [7] with a size of $33.2 \times 22.2 \text{ mm}^2$, where our proposed antenna covers all standards including these two and have a size of only $26 \times 19 \text{ mm}^2$. So comparative study shows that proposed antenna provides better outputs in terms of bandwidths, coverage and dimensions than the available antennas.

4.6 Insight into Parametric Study

In this thesis we have worked with the E shape patch antenna. In rectangular patch antenna the relation between length, L and width, W with the frequency response, bandwidth and return loss can be easily understood and realized. But in the case of E shape patch antenna, we have a lot of parameters including L and W . For instance we have already optimized the antenna by varying L , W , W_1 , L_1 and W_2 of the patch antenna. As the number of parameters increases the relations becomes very complex.

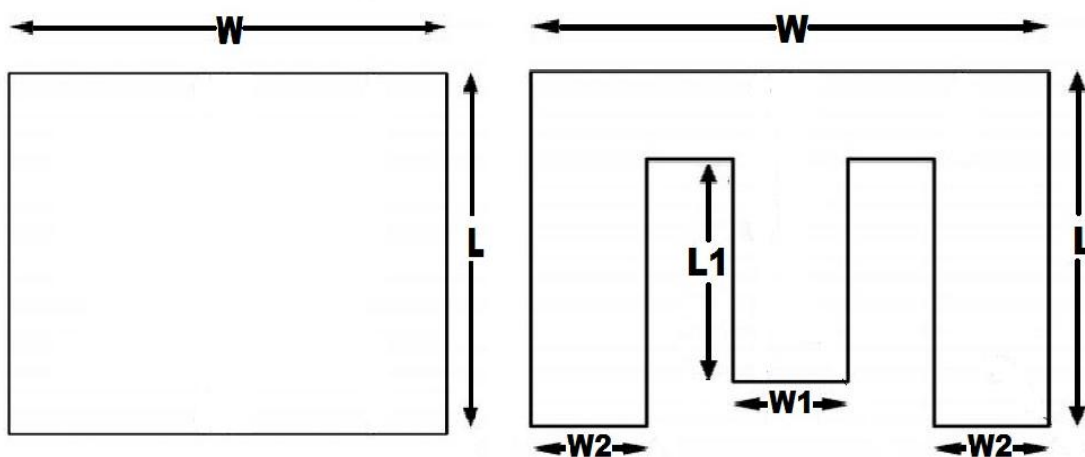


Figure 4.18: Parameters of rectangular antenna and E shaped patch antenna

We have already tried to apply empirical formulation to design our E shape antenna, but those formulas are not very accurate because our optimized design is much changed from the calculated design. So our parametric study can show effect of different parameters on the return loss, bandwidth and resonant frequency which can be very useful to optimize any E shape antenna in future.

Now the effect of various parameter changes on the return loss, frequency range and bandwidth found in this thesis are summarized in the next table.

Table 4.1. Summary of Parametric Study

	Decreasing	Parameters	Increasing
Return loss	Increasing until W=24mm	W (Original=34mm) (Final=24mm)	Decreasing
Primary Resonant Frequency	Increasing		Decreasing
Bandwidth	Slightly Increasing		Almost Similar
Return loss	Increasing until W1=5mm	W1 (Original=10mm) (Final=5mm)	Decreasing
Primary Resonant Frequency	Increasing		Decreasing
Bandwidth	Increasing until W1=5mm		Decreasing
Return loss	Decreasing	L (L=19mm)	Decreasing
Primary Resonant Frequency	Increasing		Decreasing
Bandwidth	Almost Similar		Almost Similar
Return loss	Decreasing	L1 (Original=13mm) (Final=13.94mm)	Almost Similar upto L1=14mm then decreasing
Primary Resonant Frequency	Increasing		Decreasing
Bandwidth	Almost Similar		Almost Similar
Return loss	Increasing abruptly	W2 (W2=9mm)	Decreasing Abruptly
Primary Resonant Frequency	Decreasing		Increasing
Bandwidth	Almost Similar		Almost Similar
Return loss	Increasing	Ls (Ls=13.8mm)	Decreasing
Primary Resonant Frequency	Decreasing		Increasing
Bandwidth	Decreasing		Decreasing

CHAPTER 5 CONCLUSION

In this thesis a single element, coaxial probe fed, single stacked, E shaped microstrip patch antenna has been design and optimized for a frequency band of 4.9-5.825 GHz. The antenna showed satisfactory simulation results for all the high speed WLAN standards available throughout the world. The proposed antenna showed improvement in terms of bandwidth, return loss and size from any of the existing antenna in this frequency band. A parametric study has been done to understand the effect of various parameters on the resonant frequency, return loss, gain and bandwidth. An increase in bandwidth has been achieved by which now this single antenna can be used a transceiver throughout world for many WLAN standards including IEEE 802.11a, IEEE 802.11n and IEEE 802.11j. A reduction of antenna area has been achieved as our proposed antenna needs only $26 \times 19 \text{mm}^2$ area which is much smaller than the antennas found in literature review. The results of the parametric study is summarized in table which can be used as a reference in any future works in the field of E-shaped microstrip patches.

All these optimization have performed using Zeland's IE3D electromagnetic simulation software. For future works the additional band may be removed for more precise operation only in WLAN range. Fabrication of this antenna can be performed to observe real time performance of the antenna. Further improvement can be achieved by using arrays. Using multiple layer of substrate in stacked configuration can also improve return loss and bandwidth significantly. If successful this can be produced commercially to be used in all WLAN applications throughout the globe.

APPENDIX A

RESONANCE FREQUENCY OF E- SHAPED ANTENNA

Dual-resonance frequency plays an important role in the enhancement of the bandwidth of microstrip antennas. In an E-Shaped microstrip patch antenna, two resonance frequencies are coupled to give a wide bandwidth. Hence, determination of the two resonance frequencies is an important study for the E-shaped antenna. For the determination of the resonance frequency of such an antenna, the general analysis involves using the basic electro- magnetic boundary value problem. Another way is to solve the integral equations using Green's function either in space or the spectral domain. Solution of these equations mostly uses the method of moments (MoM). During the final numerical solution, the choice of the test function and the path of integration are most critical. Thus, it involves rigorous mathematical formulation and extensive numerical procedure. Here an equivalent-area method is used to determine the resonant frequency, in which the E-Shaped antenna is converted to an equivalent rectangular microstrip antenna (RMSA) by equating its area to that of the RMSA. The results are compared with the published experimental and simulations results, which are in very good agreement with theoretical model.

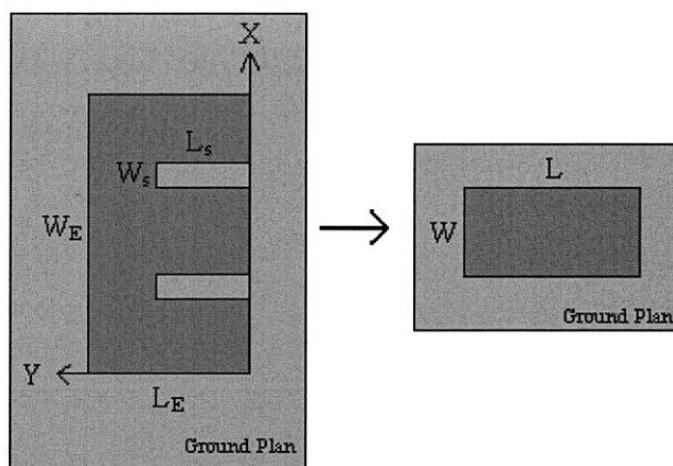


Figure A-1: Diagram for equating the area of the E-Shaped antenna with RMSA

To determine the resonance frequency at the dominant mode and higher-order modes, the area of the E-Shaped microstrip patch antenna is equated to that of a RMSA. Figure A-1 shows the E- shaped microstrip patch antenna and its equivalent RMSA.

The length L of the RMSA is taken as equal to the length of the E-shaped antenna. The width W of the RMSA is calculated as follows:

$$W = \frac{(L_E W_E - 2L_s W_s)}{L},$$

where L_E and W_E are the length and width of the E-Shaped patch antenna, respectively.

Considering width W and length L of the equivalent RMSA, the effective dielectric constants $\epsilon_{\text{eff}}(W)$ and $\epsilon_{\text{eff}}(L)$ are calculated after accounting for the dispersion effect. Now, for the equivalent RMSA with parameter h as the thickness of the substrate, ϵ_r is the dielectric constant and t is the thickness of the strip conductor, the frequency dependent formula used for the computation of effective dielectric constant $\epsilon_{\text{eff}}(W)$ is calculated as

$$\epsilon_{\text{eff}}(W) = \epsilon_r - [(\epsilon_r - \epsilon_{\text{eff}}(0))/(1 + P)],$$

where $\epsilon_{\text{eff}}(0)$ is the static effective dielectric constant, given by

$$\epsilon_{\text{eff}}(0) = \frac{1}{2} \{(\epsilon_r + 1 + (\epsilon_r - 1)G)\},$$

$$G = (1 + 10h/W)^{-AB} - [(\ln 4/\pi)(t(Wh)^{-1/2})],$$

$$A = 1 + \left\{ \frac{(Wh)^4 + W^2/(52h)^2}{(Wh)^4 + 0.432} \right\} + \frac{1}{18.7} \ln\{1 + [W/(18.1h)]^3\},$$

$$B = 0.564 \exp[-0.2/(\epsilon_r + 0.3)].$$

$$P = P_1 P_2 [(0.1844 + P_3 P_4) f_n]^{1.5763},$$

$$P_1 = 0.27488 + [0.6315 + \{0.525/(1 + 0.0157f_n)^{20}\}]u - 0.065683 \exp(-8.7513u),$$

$$P_2 = 0.33622[1 - \exp(-0.03442\epsilon_r)],$$

$$P_3 = 0.0363 \exp(-4.6u)\{1 - \exp[-(f_n/38.7)^{4.97}]\},$$

$$P_4 = 1 + 2.751\{1 - \exp[-(\epsilon_r/15.916)^8]\},$$

$$f_n = 47.713kh, \quad \text{where } k = 2\pi/\lambda_0,$$

$$u = [W + (dW - W)/\epsilon_r]/h,$$

$$dW = W + (t/\pi)[1 + \ln\{4/(t/h)^{1/2} + (1/\pi)^2/(W/t + 1.1)^2\}].$$

The effective dielectric constant $\epsilon_{\text{eff}}(L)$ corresponding to width equal to L , is computed by replacing W with L in all above equations. The effective dielectric

constant is calculated using

$$\varepsilon_{eff}(f) = [\varepsilon_{eff}(W)\varepsilon_{eff}(L)]^{1/2}.$$

The effective width W_{eff} and effective length L_{eff} of the equivalent RMSA is calculated as follows

$$W_{eff} = W + 2\Delta l_1,$$

$$L_{eff} = L + 2\Delta l_2,$$

where Δl_1 and Δl_2 are edge extensions of side L and W of the equivalent RMSA respectively, and are calculated using $\varepsilon_{eff}(L)$ and $\varepsilon_{eff}(W)$. The edge extension Δl_2 for the width W of the equivalent RMSA is determined in a similar way as [16]:

where

$$\xi_1 = 0.434907 \frac{\varepsilon_{eff}(W)^{0.81} + 0.26(W/h)^{0.8544} + 0.236}{\varepsilon_{eff}(W)^{0.81} - 0.189(W/h)^{0.8544} + 0.87},$$

$$\xi_2 = 1 + \frac{(W/h)^{0.371}}{2.358\varepsilon_r + 1},$$

$$\xi_3 = 0.434907 \frac{\varepsilon_{eff}(W)^{0.81} + 0.26(W/h)^{0.8544} + 0.236}{W^{0.81} - 0.189(W/h)^{0.8544} + 20.1167},$$

$$\xi_4 = 1 + 0.0377 \arctan[0.067(W/h)^{1.456}] \times [6 - 5 \exp\{0.036(1 - \varepsilon_r)\}],$$

$$\xi_5 = 1 - 0.218 \exp(-7.5W/h).$$

Similarly, Δl_1 is calculated by replacing W by L and $\varepsilon_{eff}(W)$ by $\varepsilon_{eff}(L)$ in above equations. Using the all the equations, the resonance frequency for E-shaped microstrip antenna is calculated as, the lower resonance frequency : [17]:

$$f_{lower} = \frac{v_0}{2l_{eff}\sqrt{\varepsilon_{eff}}}.$$

and the higher frequency of E-shaped microstrip antenna, formula is modified appropriately as

$$f_{higher} = \left(\frac{0.36v_0}{W_{eff}\sqrt{\varepsilon_{eff}}} \right),$$

where v_0 is the velocity of light in free space.

APPENDIX B

ANTENNA SIMULATION IN IE3D

Step by step procedure to design an E shape patch antenna with dimensions = 34 mm, L = 19 mm, W1 = 10 mm, W2 = 9 mm, L1 = 13 mm and Ls = 13.8 mm is discussed here with corresponding screenshots.

1. Run Zeland Program Manager. Click on MGRID.

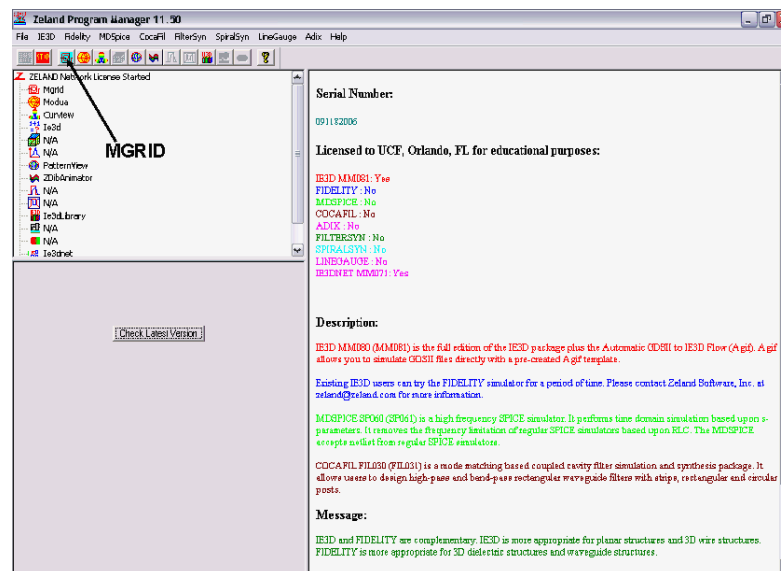


Figure B-1: Zeland Program Manager

2. MGRID window opens. Click the new button as shown below (□).

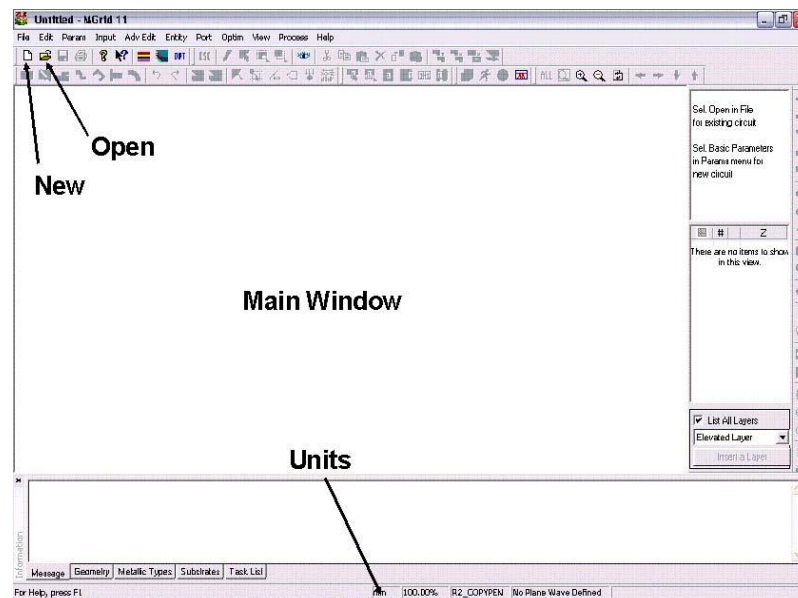


Figure B-2: MGRID window

3. The basic parameter definition window pops up. In this window basic parameters of the simulation such as the dielectric constant of different layers, the units and layout dimensions, and metal types among other parameters can be defined by users. In “Substrate Layer” section two layers are automatically defined. At $z=0$, the program automatically places an infinite ground plane (note the material conductivity at $z = 0$) and a second layer is defined at infinity with the dielectric constant of 1.

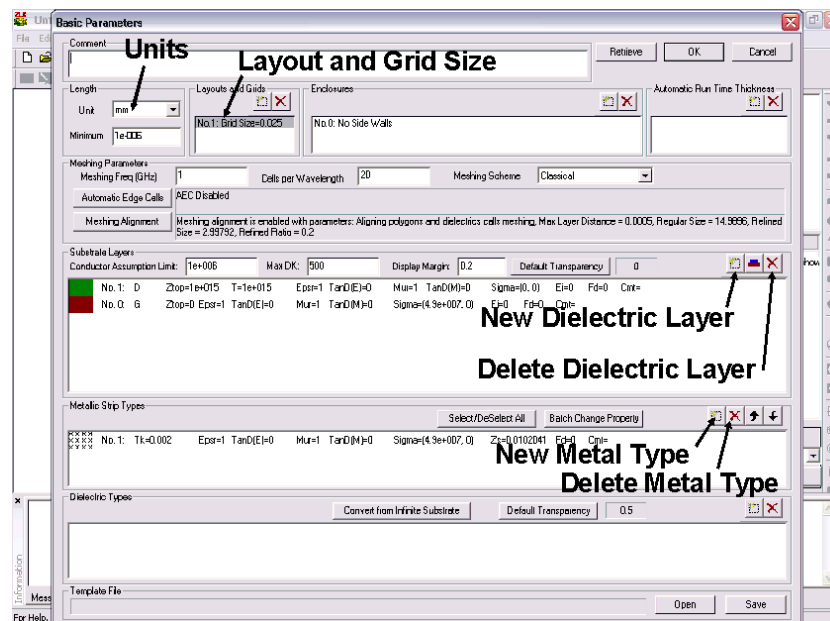



Figure B-3: Basic Parameter

4. Click on “New Dielectric Layer” button (). Enter the basic dielectric parameters in this window: Ztop: 5; Dielectric Constant: 2.2, Loss tangent: 0.002. Click OK.

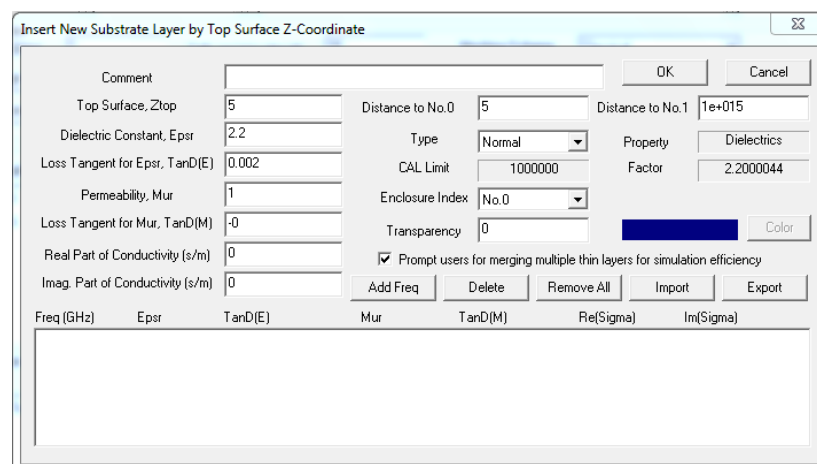


Figure B-4: New Substrate Layer Dialog box

- Click OK again to go back to MGRID window. In Menu bar click Entity>Rectangle. Rectangle window pops up, enter Length 34, width 3 and click OK,

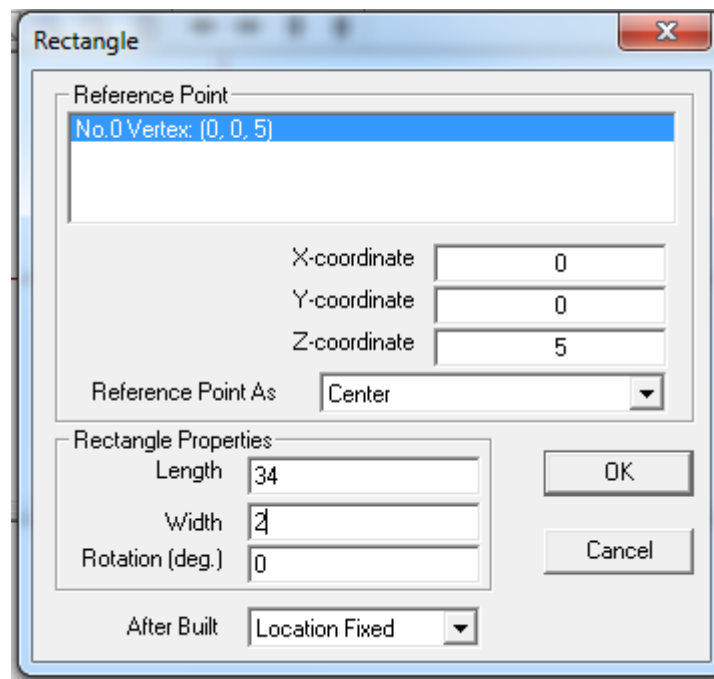


Figure B-5: Rectangle Dialog box

- Click ALL button to see the whole structure. Select two lower vertices. Click Adv Edit>Continue Straight Path. Continue Path on Edge window pops up. Enter Path Length 13, Path Start Width 10, Click OK.

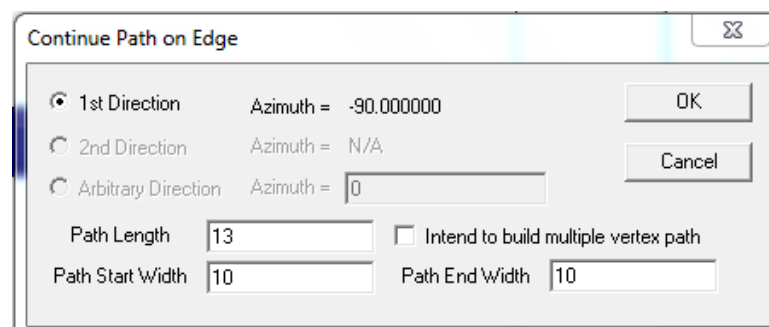


Figure B-6: Continue Straight Path Dialog box

- Click ALL to see the whole structure. The main body with the middle arm has been created.

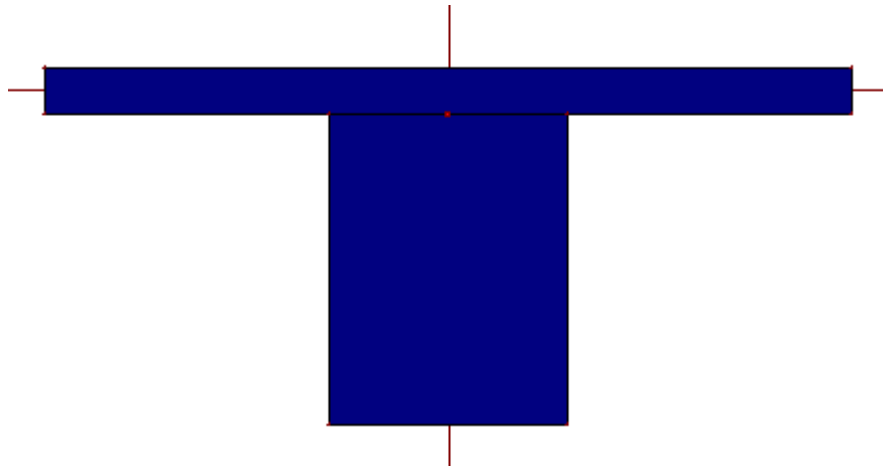


Figure B-7: Main body of antenna with middle arm

8. Click Input>Key In Absolute Location. New window pops up, enter X coordinate -17, Y coordinate -1.5. Click OK. Program would ask to connect, always click YES. Then click Input>Key In Relative Location. Another window pops up, enter X coordinate 9, Y coordinate 0. Click OK. Then again click Input>Key In Relative Location and enter X coordinate 0, Y coordinate -17. Click OK. Press Shift+F or Input>Form Rectangle. Leftside arm of the E has now been created.

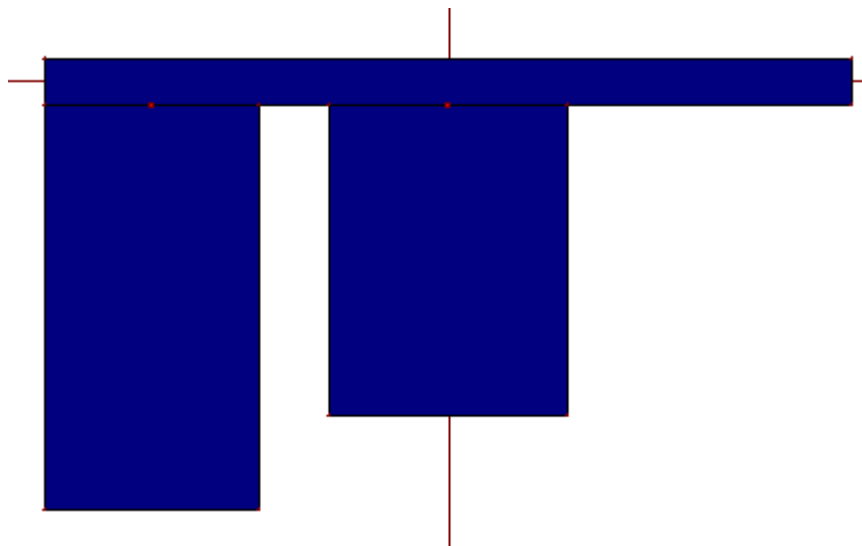


Figure B-8: Antenna Structure with two arms

9. Now click Edit>Select Polygon, click on the left arm. Right click on it, from the menu click Copy. Click right mouse button it anywhere in the MGRID panel and

click Paste. Click again in the panel. A window pops up. Enter X offset 25, Y offset 0, Click Ok. Antenna structure is now complete. Next we need to connect the feed line to the antenna.

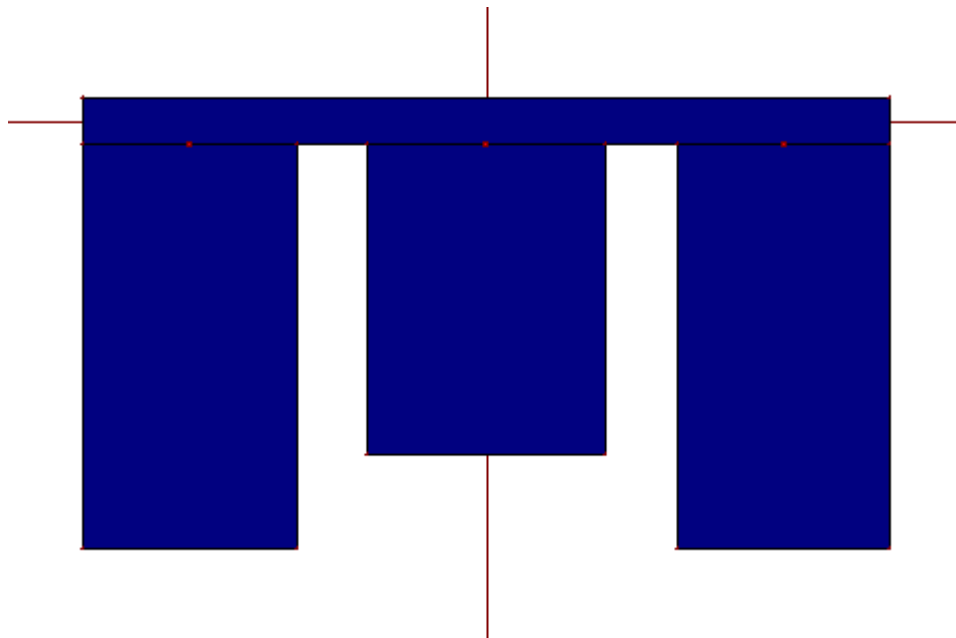


Figure B-9: Complete antenna structure

10. Click Entity>Probe Feed to Patch. Enter (0, -12.8) as feed coordinate and click OK. The antenna is now ready for simulation.

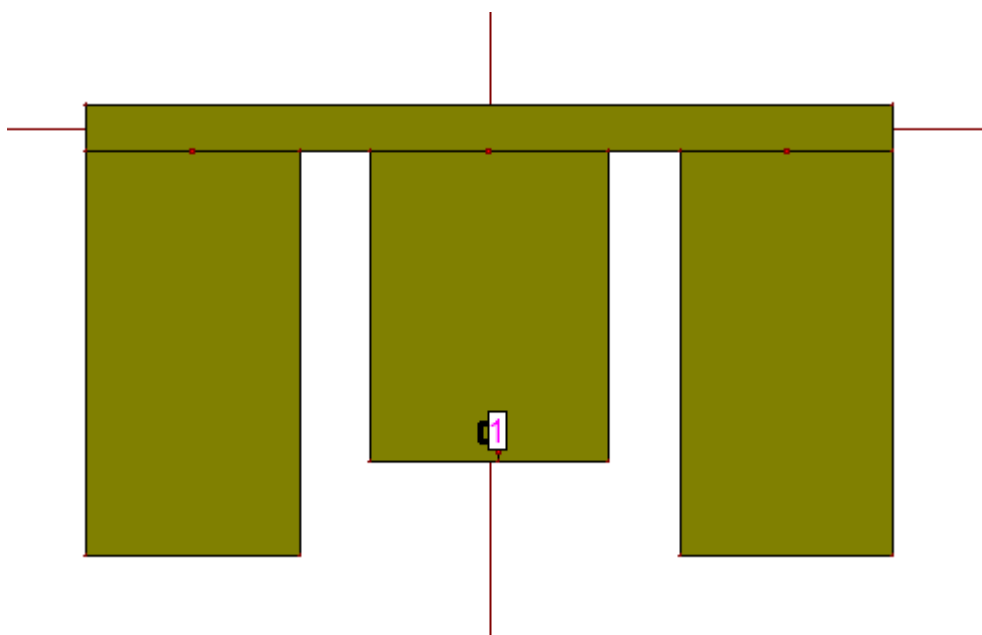


Figure B-10: Antenna Structure with feeding Probe

APPENDIX C

MESHING PARAMETERS AND SIMULATION

For simulation of the antenna, first meshing should be performed. In IE3D this meshing is used in the Method of Moment (MoM) calculation. Click on Process>Display Meshing. The “Automatic Meshing Parameters” menu pops up.

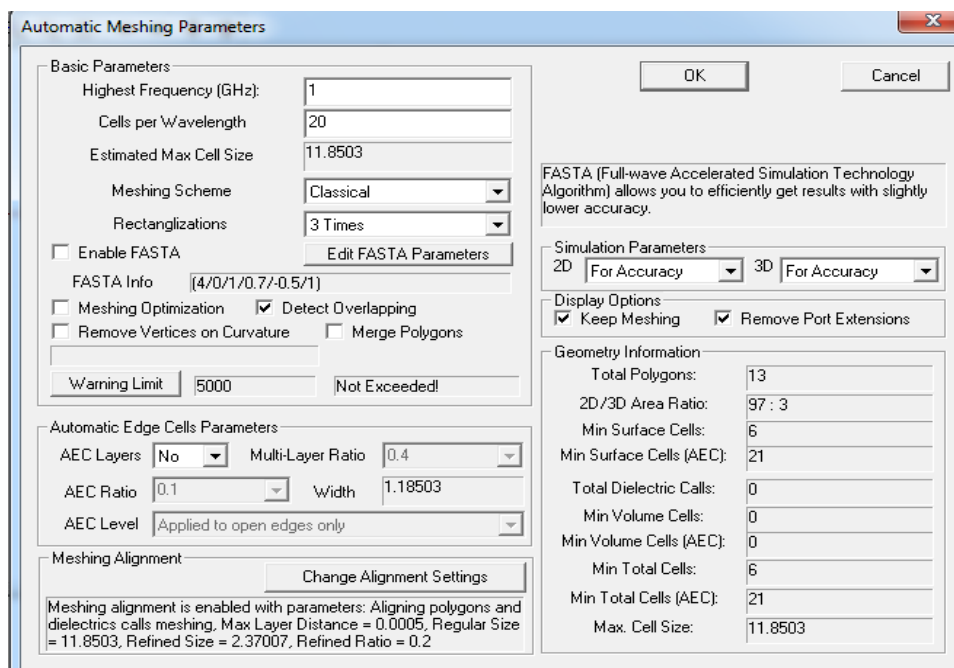


Figure C-1: Automatic Meshing Parameter dialog box

Here the highest frequency is should be defined as the maximum operating frequency. In this thesis simulations are done with 9 GHz in the “Highest Frequency” field and 30 in the “Cells per Wavelength” field. The number of cells/wavelength determines the density of the mesh. In method of moment simulations, fewer than 10 cells per wavelength should not be used. The higher the number of cells per wavelength, the higher the accuracy of the simulation. However, increasing the number of cells increases the total simulation time and the memory required for simulating the structure. In most of the simulations using 20 to 30 cells per wavelength should provide enough accuracy. However, this cannot usually be generalized and is different in each problem; press OK, a new window pops up that shows the statistics of the mesh; press OK again and the structure will be meshed.

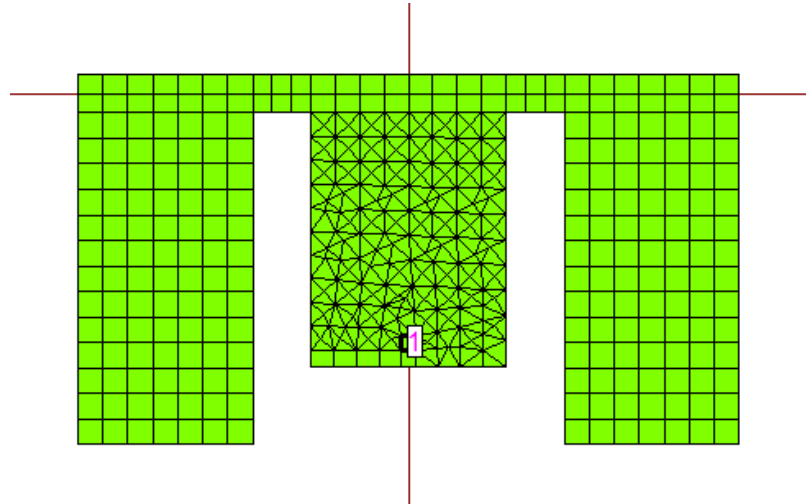


Figure C-2: Meshed Antenna for MoM calculation

Now to get S11 parameters of the antenna, Click on Process>Simulate. Simulation Setup window pops up. Here range of frequency should be entered as 3 GHz to 7 GHz with 0.01 in the Step Hertz field.

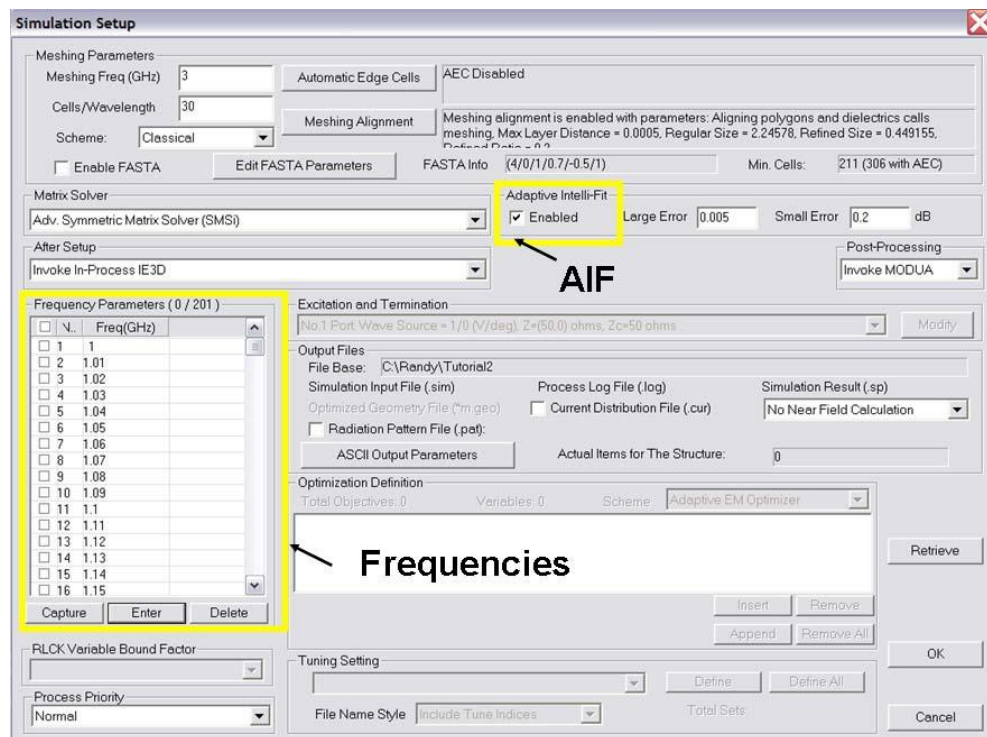


Figure C-3: Simulation Setup dialog box

The “Adaptive Intelli-Fit” check box should be checked so that the program does not perform simulations at all of the specified frequency points. It

automatically selects a number of frequency points and simulates the structure at these particular points and interpolates the response based on the simulated points. Press OK and the structure will be simulated. The simulation progress window shows the progress of the simulation. It will only take a couple of seconds for the simulation to finish. After the simulation is completed, IE3D automatically invoked MODUA and shows the S parameters of the simulated structure. MODUA is a separate program that comes with the IE3D package. This program is used to post process the S-parameters of the simulated structure.

From the Control Menu of MODUA the display graph can be defined. Click Control>Define Display Graph. Display Parameter window pops up with many option. Any needed data can be chosen for display.

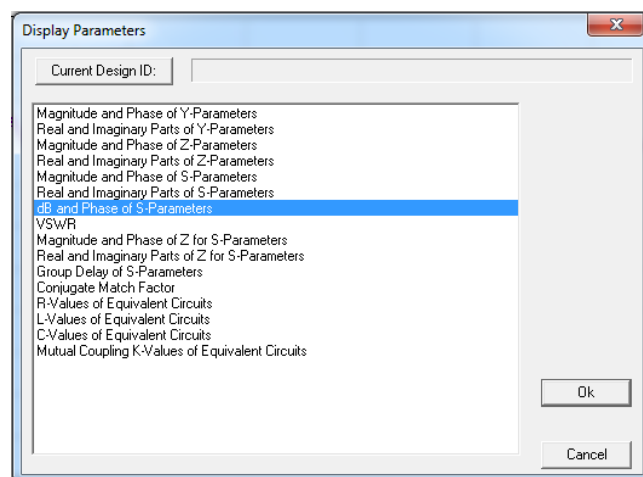


Figure C-4: Display Parameter

For simulation of the current distribution and radiation pattern, Simulation Setup dialog should be modified. Cell per wavelength should be higher for better accuracy; a value of 50 to 70 is enough. A single frequency should be given for which current distribution or radiation pattern would be observed and current distribution file check box must be checked.

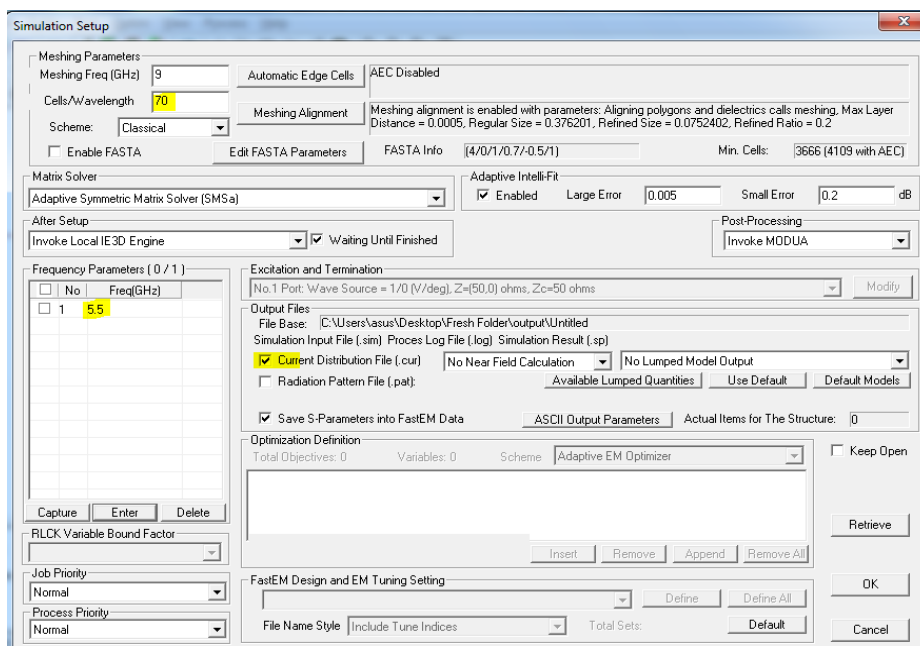


Figure C-5: Simulation Setup parameters for Current Distribution and Radiation Pattern

REFERENCES

- [1] Pozar, D. M., "Micro-strip antenna coupled to a micro-strip-line," *Electron. Letter*, vol. 21, no. 2, pp. 49–50, Jan. 1985.
- [2] Lee, K. F., et al., "Experimental and simulation studies of the coaxially fed U-slots rectangular patch antenna," *IEE Proc. Microw. Antenna Propagation*, Vol. 144, No. 5, 354–358, October 1997.
- [3] Chair, R., Mak, C. L., Lee, K. F., Luk, K. M. , Kishk, A. A., "Miniature Wide-Band Half U-Slot and Half E-Shaped Patch Antennas," *IEEE Transactions on Antennas and Propagation*, Vol. 53, No. 8, pp. 2645-2652, August 2005.
- [4] Rafi, G. and L. Shafai, "Broadband micro-strip patch antenna with V-slot," *IEE Proc. Microw. Antenna Propagation*, Vol. 151, No. 5, 435–440, October 200A-
- [5] M. Sanad, "Double C-patch antennas having different aperture shapes," in *Proc. IEEE AP-S Symp.*, Newport Beach, CA, June 1995, pp. 2116–2119.
- [6] Yang, F., X. X. Zhang, X. Ye, and Y. Rahmat-Samii, "Wide-band E-shaped patch antennas for wireless communications," *IEEE Trans. Antennas Propagat.*, Vol. 49, No. 7, 1094–1100, July 2001.
- [7] Ge, Y., K. P. Esselle, and T. S. Bird, "A compact E-shaped patch antenna with corrugated wings," *IEEE Trans. Antennas Propagation*, Vol. 54, No. 8, 2411–2413, Aug. 2006.
- [8] Yu, A. and X. X. Zhang, "A method to enhance the bandwidth of micro-strip antennas using a modified E-shaped patch," *Proceedings of Radio and Wireless Conference*, 261–264, Aug. 10–13, 2003.
- [9] Khidre, A., Lee, K. F., Yang, F., and Eisherbeni, A., "Wideband Circularly Polarized E-Shaped Patch Antenna for Wireless Applications", *IEEE Antennas and Propagation Magazine*, Vol. 52, No.5, October 2010. pp. 219-229.

- [10] Sim, C. Y. D., J. S. Row, and Y. Y. Liou, "Experimental studies of a shorted triangular micro-strip antenna embedded with dual V-shaped slots," *Journal of Electromagnetic Waves and Applications*, Vol. 21, No. 1, 15–24, 2007.
- [11] Kaizhong Zhan, Qinggong Quo, and Kama Huang, "A novel kind of Bluetooth and UWB antenna," 2010 International Conference on Microwave and Millimeter Wave Technology (ICMMT), pp. 1038 - 1041.
- [12] Yikai Chen, Shiwen Yang, and Zaiping Nie, "Bandwidth Enhancement Method for Low Profile E-Shaped Microstrip Patch Antennas," *IEEE Transactions on Antennas and Propagation*, vol. 58, no. 7, pp. 2442 - 2447, 2010.
- [13] Online: <http://www.antenna-theory.com>.
- [14] Balanis, C. A.; "Antenna Theory: Analysis and Design", John Wiley & Sons, Publishers, Inc. 1997, New York.
- [15] Tsoulos, G. V.; "Adaptive antennas for wireless communications", IEEE Press, 2001, USA.
- [16] Garg, R.; Reddy, V.S.; , "A broad-band coupled-strips microstrip antenna," *IEEE Transactions on Antennas and Propagation*, , vol.49, no.9, pp.1344-1345, Sep 2001
- [17] W. L. Stutzman and G. A. Thiele, *Antenna Theory and Design*, 2nd edition, John Wiley & Sons, Inc., 1998.
- [18] Chang, E.; Long, S.; Richards, W.; , "The resonant frequency of electrically thick rectangular microstrip antennas," *Antennas and Propagation Society International Symposium*, 1986 , vol.24, no., pp. 883- 886, Jun 1986.
- [19] Hyung-Gi Na; Hyo-Tae Kim; , "Electromagnetic scattering from eccentric multilayered dielectric bodies of revolution-numerical solution," *Antennas and Propagation*, *IEEE Transactions on* , vol.44, no.3, pp.295-301, Mar 1996
- [20] Zeland IE3D: MoM-Based EM Simulator 14.1 User manual.

- [21] Matin, M.A.; Ali, M.A.M.; “Design of broadband stacked E-shaped patch antenna,” International Conference on Microwave and Millimeter Wave Technology (ICMMT 2008), vol.4, pp.1662-1663, 21-24 April 2008.
- [22] Singh, A.; “Dual band E-shaped patch antenna (ESPA) for ultra wide band applications,” Asia Pacific Microwave Conference (APMC 2009), pp.2770-2773, 7-10 Dec. 2009.
- [23] D. K. Neog, S. S. Pattnaik, D. C. Panda, S. Devi, Malay Dutta and O. P. Bajpai, “New Expression for the resonance frequency of an E-shaped Microstrip Antenna,” Wiley periodicals on Microwave and optical technology letters, Vol. 48, No. 8, pp.1561-1563, August 2006.